D.P. REPORT 473

O.E.C.D. HIGH TEMPERATURE REACTOR PROJECT

DRAGON

Dragon Project Report

DIMENSIONAL CHANGES IN GRAPHITE DURING HIGH TEMPERATURE IRRADIATION IN THE HIGH FLUX REACTOR RCN, PETTEN

by

R. BLACKSTONE – Reactor Centrum Nederland, Petten, Holland.

L. W. GRAHAM – Dragon Project.

A.E.E. Winfrith, Dorchester, Dorset, England

July, 1967

DISCLAIMER

DIMENSIONAL CHANGES IN GRAPHITE DURING HIGH TEMPERATURE IRRADIATION IN THE HIGH FLUX REACTOR RCN, PETTEN

by

R. BLACKSTONE - Reactor Centrum Nederland,
Petten, Holland

L. W. GRAHAM - Dragon Project

ABSTRACT

The dimensional changes observed in a range of graphitic materials following irradiation at 600, 900 and 1200°C are reported. The results are discussed in the light of current models for irradiation damage in graphite and it is concluded that for conventional materials the dimensional behaviour can be related to the material properties.

Further confirmation of the extreme dependence of the dimensional changes on the crystallite size has been obtained. The way in which the rate of dimensional change varies with temperature is compatible with this effect being caused by vacancy loss at crystallite boundaries. For a given crystallite size there appears to be a breakaway temperature above which the rate of dimensional change accelerates rapidly.

Evidence has been found which indicates that even for low doses at high temperatures, the rate of shape change in the crystals (and hence the bulk dimensional changes) are also significantly affected by the mechanical deformation of the crystallites under irradiation conditions (irradiation creep). Young's modulus has been used as an index of this effect: in materials with low modulii (i.e., more easily deformed) the crystallite shape change produced by irradiation is opposed by basal plane shear. On the other hand the dimensional changes in materials of high Young's modulus (i.e., stiffer crystals) are larger than expected because the crystallite shape change is less easily opposed.

Because of these effects the role of the coefficient of expansion as a parameter in correlating irradiation behaviour in different materials is somewhat limited.

The report concludes with a discussion of the properties required of graphite for use in HTGCR's in the context of the environment in these reactors.

CONTENTS

LIST OF TABLES

Page No.

TABLE

LIST OF ILLUSTRATIONS

FIGURE

FIGURE

DIMENSIONAL CHANGES IN GRAPHITE DURING HIGH TEMPERATURE IRRADIATION IN THE HIGH FLUX REACTOR RCN, PETTEN

by

R. BLACKSTONE

L. W. GRAHAM

1. INTRODUCTION

In 1962 work commenced on the design of a graphite irradiation capsule for a small programme of testing in the HFR at Reactor Centrum Nederland, Holland. Initially the work had the very limited aim of providing data on the materials being used in the construction of the Dragon Reactor. The capsule, which has now operated successfully for a number of years is unique in design having three separately controlled electrically heated zones operating at 600, 900 and 1200°C.

With the successful development of coated particle fuels and the important role which graphite is required to play in economically attractive power reactors based on their use, the programme has continued and is now much wider in scope. The capsule experiments are now operated by RCN jointly for the Dragon Project, the THTR Project and Euratom. Complete details of the work to date will be given in a separate report [1]. The purpose of the present work is to review the effects found in studying dimensional changes produced in graphite by fast neutron irradiation in view of the importance of this subject in the design of High Temperature Gas Cooled Reactors.

The report is in several parts. Because of the apparent complexity of the subject a simplified mechanism is first set out to aid in the rational discussion of the work. After briefly summarising the experimental methods the results are first presented and then discussed. Some main conclusions are drawn and finally the report concludes with a section on the specification and behaviour of graphite in high temperature power reactors.

2. MECHANISM OF IRRADIATION INDUCED DIMENSIONAL CHANGES

The first results obtained from the Dragon irradiation experiments at 600, 900 and 1200°C in the HFR Petten were interpreted as indicating that the irradiation damage model developed by Simmons, Nettley and their co-workers [2, 3] for lower temperatures could be extended to explain the effects of irradiating at higher temperatures. To aid in the rational discussion of the results now given, a model is first described: this model is the authors' interpretation of that developed in the UK. For ease of presentation a much wider temperature range than covered in the experimental work is discussed.

2.1 Damage in Individual Crystallites

The collision of fast neutrons with carbon atoms in graphite crystals produces high energy carbon atoms which in turn collide with other carbon atoms forming interstitials and vacancies. Most of the interstitials and vacancies quickly recombine. At low temperatures the vacancies which are not annihilated are initially isolated single sites which are

not mobile: on the other hand the interstitials which do not immediately react with vacancies, quickly combine into small mobile groups. These mobile groups nucleate into larger clusters the size of which increases with increasing temperature of irradiation. The presence of interstitial clusters of a range of sizes between the layer planes causes the planes to be forced apart and leads to an expansion in the crystallite c-direction. Additionally there is a contraction in the crystallite a-direction which can vary in magnitude relative to the c-direction expansion according to the circumstances:

(a) At low temperatures where vacancies are immobile, the presence of single vacancies (coupled with expansive effects in the c-direction due to interstitials) may lead to slight collapse in the a-direction due to the contraction of the carbon skeleton about the vacancy due to a change in C-C bond order. Alternatively an a-direction shrinkage could be caused by visualising no such collapse but a puckering of the layer planes or even a Poisson's ratio effect.

(b) With increasing dose, lines of vacancies may form by random juxtaposition, each line collapsing when its length exceeds a critical size [4].

(c) If the temperature is sufficiently high, vacancies will become mobile. This may lead to the onset of line vacancy formation and collapse at lower doses. Alternatively two other fates become possible: the clustering of vacancies into plates rather than lines, leading to less complete collapse in the a-direction; or the loss of vacancies at crystallite edges which enhances the a-direction shrinkage. It is believed that as the vacancy mobility increases, with the result that the single vacancy concentration becomes smaller, the chances for vacancy-interstitial annihilation diminish so that the c-axis crystallite expansion rates increase.

An attempt to summarise the effects of these displacements on the crystallite dimensions at different temperatures is made in Fig. 1. It should be stated that at this point that the term crystallite refers to that volume of the material which behaves as a unit during the irradiation. The crystallites to which Fig. 1 is meant to apply would be those present in well-graphitised conventional nuclear graphite exemplified by Pile Grade A. In Fig. 1 the rate of growth for unit neutron dose has been plotted for the c-direction $\left(g_c\right)$ and the a-direction $\left(g_a\right)$, the former always exhibiting an expansion and the latter always a shrinkage.

The crystallite volume changes produced by the interstitial and vacancy defects are important in the discussion of dimensional changes in bulk materials. The following ranges are postulated.

(i) Up to about 300°C but decreasing in magnitude as this temperature is approached, the high population of small sized

groups of interstitials and single vacancies leads to a large volume increase.

(ii) In the range 300°C to about 450°C large interstitial clusters and collapsed vacancy lines produce crystal shape change at substantially constant volume.

(iii) The crystallite volume again increases with irradiation in the temperature range 500°C to about 1000°C because vacancy diffusion and clustering now occurs, thus reducing the a-direction collapse.

(iv) Above say 1000°C, when vacancy mobility becomes increasingly greater, the probability of vacancy loss at crystallite boundaries is enhanced and a state of crystallite shape change at constant volume may once again be found.

2.2 Effect of Crystallite Size

Variations in crystallite size would be expected to produce important differences in crystallite behaviour. In particular at high temperatures a decrease in the effective crystallite diameter reduces the diffusion distance required for vacancy loss at the crystallite boundaries. Thus at temperatures where vacancy diffusion is significant the shape-change in small crystallites would occur at a greater rate than in large crystallites since in the latter case there would be a greater probability of vacancy-interstitial reaction (and also vacancy clustering). This can also be visualised as a higher effective irradiation temperature for smaller crystallite size.

2.3 Effect of Dose

It should be emphasized that there is no reason to suppose that the crystals will reach a state of dimensional stability at a sufficiently high neutron dose. Thus at high temperatures the growth of interstitial clusters may be visualised as the progressive enlargement of new layer planes inserted into the crystals, leading to crystal growth in the c-direction and shrinkage in the a-direction. This process could continue indefinitely in an unrestrained crystal, the new layer planes themselves becoming damaged by the same process.

The rates of dimensional change g_c and g_a in the crystallite c-direction and a-direction respectively may also vary as a function of dose. For example, the onset of the formation and collapse of line vacancies, which is dependent on the statistical probability of producing vacancies in adjacent lattice points, leads to an acceleration in the rates of dimensional change in both crystallite directions.

2.4 Dimensional Changes in Polycrystalline Graphites

In a polycrystalline graphite of theoretical density and also completely oriented, the bulk dimensional changes of the material on

irradiation would be identical to those occurring in the individual crystallites.

However, in materials of practical interest the bulk density is usually far removed from that of the crystallites and the preferred orientation can vary over a wide range.

Porosity in the graphite may be loosely classified into macroscopic and microscopic. For the purpose of discussing irradiation effects the important microporosity may be identified with fissures existing in the crystallites and lying parallel to the a-direction. These are formed when the material is cooled from the heat-treatment or graphitising temperature as a result of the relief of stresses brought about by the extreme anisotropy in the properties of the graphite crystal.

In "real" materials the observed effects of irradiation on the bulk dimensional changes are profoundly affected by the degree of preferred orientation and the average frequency and size of microcracks. These parameters affect the degree by which the crystallite dimensional changes are transmitted to any given direction in the bulk material. In particular the c-direction expansion caused by interstitial clusters is partially absorbed by the microcracks. With progressive increases in the irradiation dose, crack closure occurs and causes dramatic changes in the bulk dimensional changes.

These effects may be analysed quantitatively in relation to the crystallite dimensional changes by using the expression:

$$R_x = A_x g_c + (1 - A) g_a \qquad (1)$$

where R_x is the rate of dimensional change in the material in the x-direction, and g_c and g_a are the previously defined crystallite dimensional changes. In the case of irradiation specimens the directions of cut are usually either parallel or perpendicular to the direction of forming. The parameter A_x essentially describes the proportion of the crystallite dimensional change which is transmitted to the bulk. As discussed above, A_x is initially dependent on the degree of preferred orientation and on the degree by which the microcracks attenuate the c-direction expansion.

In its simplest form the model relates the irradiation induced dimensional changes to similar effects occurring when the crystallites are strained thermally. Thus the thermal expansion in the x-direction (α_x) is related to the thermal expansion in the crystallites in the c and a-directions $(\alpha_c$ and $\alpha_a)$ by an expression:

$$\alpha_x = A_x \alpha_c + (1 - A_x) \alpha_a \qquad (2)$$

That is, the crystallite thermal and irradiation induced strains are transmitted to the bulk through identical couplings, A_x being the same

value in equations (1) and (2). In principle then, the crystallite dimensional changes may be determined by measuring the bulk dimensional changes and the way in which the coefficient of thermal expansion varies as a function of neutron dose.

In the case of a typical anisotropic graphite being irradiated at a temperature where the crystallite volume is substantially constant, the type of dimensional behaviour expected is illustrated in Fig. 2a. In the direction parallel to extrusion a continuous shrinkage occurs, since this direction is mainly governed by the a-direction of the crystallites. Initially a shrinkage is observed in the perpendicular direction also, even though a major fraction of the crystallite c-direction expansion is occurring in this direction. This is because the expansion is accommodated by the oriented microporosity. However, as the microcracks close, the rate of shrinkage diminishes and eventually an expansion occurs. Clearly for maximum stability under conditions where the crystal volume remains constant, i.e., when $g_c = -2g_a$, then it is required that:

(i) the parameter A in equation (1) is the same in all directions in the material

(ii) the value of A should be $\frac{1}{3}$ since at constant volume in the crystallites $g_c = -2g_a$ and $R_x = 0$.

The correlation between the coefficient of expansion and irradiation growth indicates that for the above to be attained the material would have to be completely isotropic in terms of its thermal expansion properties and the coefficient of thermal expansion approach a value $\frac{1}{3}$ of that of the volume coefficient of the crystallite, i.e., about $9 \times 10^{-6}/°C$. Although this level of expansion coefficient is obtainable in principle, the most advanced economically practical materials exhibit coefficients of expansion of about $5 \times 10^{-6}/°C$, i.e., microporosity is present which can accommodate c-direction expansion. Initially, as shown in Fig. 2b, a shrinkage is observed but this decreases in rate with increasing dose and a state of near stability is reached when the crack closure is complete. As before it is assumed that the crystallites change shape at constant volume.

For cases in which the crystallite volume increases as a result of irradiation, dimensional stability is never achieved and behaviour illustrated in Fig. 2c might be expected in an isotropic graphite.

2.5 Application and Development of the Model

The model outlined in the previous sections has been developed with qualified success in a quantitative manner for irradiation temperatures up to about 650°C: most of this work has been concentrated on one material (Pile Grade A graphite). However, the application of the principles of the model have led to the formulation of a guiding specification for graphites possessing improved dimensional stability

in the temperature range 300-650°C. Irradiation of such materials has shown that the application of the model is successful in general at these low temperatures.

However, effects have been found at high doses which require modification of the model. In particular it has been found that at sufficiently high doses, the changes observed in the coefficient of thermal expansion following irradiation are not compatible with the dimensional changes observed: i.e., the parameter A in equations (1) and (2) is no longer the same for conditions of irradiation and thermally induced straining [5].

This is not surprising since the equality is essentially dependent on the existence of the microcracks which lead to the effects being controlled by geometrical factors. At high irradiation doses, when these cracks are tightly closed, the restraints on the crystals are modified. Furthermore, these restraints are not likely to be the same for thermal expansion as for irradiation growth. Specifically, irradiation creep in graphite is known to occur and thus the way in which the crystallites deform by this process under conditions of mutual restraint will not be reflected in the thermal expansion measurement made outside the irradiation environment.

The degree by which accommodation due to irradiation creep affects the bulk dimensional changes seems, on the present evidence, to depend on the isotropy of the grist particles. In particular, graphites made from anisotropic grist particles exhibit volume increases after crack closure has occurred. This increase appears to be caused by the generation of a new family of cracks. After the closure of the initially present oriented porosity it seems that crystal strain can continue to be accommodated only by the generation of new porosity. This, presumably, is because the irradiation creep process occurs by a mechanism that does not allow material movement on such a scale as to fill the voids produced by the crystal deformation. It is found that when irradiated to very high neutron doses at 350-450°C* PGA graphite exhibits a change in dimensions very like that shown in Fig. 2a [5]. Thus the high dose behaviour does not differ grossly from that indicated by the original model but there are two important quantitative differences suggested by the most recently published data:

(1) the dimensional behaviour during irradiation cannot be related to changes occurring in the coefficient of thermal expansion

(2) porosity is generated at high irradiation doses.

On the other hand, data published for the same irradiation conditions but referring to a graphite made from "more nearly isotropic" grist particles than PGA graphite, seem to suggest that this graphite exhibits negligible porosity generation at high doses, i.e., for these particular conditions Fig. 2b applies.

---

*At this temperature the crystallites are expected to change shape at constant volume.

In the context of the graphite crystal, isotropic grist particles can only mean that these are spherical, with the graphite basal planes lying on concentric spheres. Further, the fact that porosity generation was negligible relative to the anisotropic grist material after the tight closure of the accommodation porosity, suggests that the creep process is probably associated with the sliding and collapse of the layer planes under the conditions of substantially hydrostatic restraint in the case of spherical grist particles. It is difficult, however, to visualise the behaviour of these spherical grist particles at high doses under conditions where the crystallite volume increases, in other words, of a sphere of which the volume increases and the surface area decreases. In fact in that case the creep process must have a volume effect or else the particle will probably break up into non-spherical and thus anisotropic parts.

However, it should be emphasised that these findings refer to low temperatures only (ca. 350-450°C): results for higher temperatures might well be affected by changes in the irradiation creep behaviour or by a tendency for vacancy diffusion to alter the crystallite volume changes.

3. EXPERIMENTAL DETAILS

Full details about the experiment are given in a separate report [1]. Only the most essential points are mentioned here.

(1) The irradiations were carried out in the core of the High Flux Reactor, HFR, at Petten, The Netherlands.

(2) A fully instrumented capsule was used with three temperature regions, controlled at 600, 900 and 1200°C respectively. The fast flux density in the capsule ranged from 0.9×10^{14} n cm^{-2} s^{-1} to 0.4×10^{14} n cm^{-2} s^{-1} depending on the position in the capsule.

(3) The neutron exposures are measured by activation of nickel and cobalt, making use of the activation reactions Ni-58 (n,p) Co-58 and Co-59 (n,γ) for the calculation of the fast and thermal flux density respectively. The values of the integrated fast flux used throughout this report are given in terms of an equivalent integrated fission flux. For comparison of results with those obtained in UK reactors, especially DIDO and PLUTO at Harwell, present evidence suggests that all neutron exposures quoted here have to be multiplied by a factor 1.75, i.e., 1.00×10^{20} n cm^{-2} Petten = 1.75×10^{20} n cm^{-2} UK [6].

(4) For the bulk synthetic graphites specimens were cut parallel (//) or perpendicular ($\perp$) with respect to the axis of forming (extrusion or pressing). The specimens had the following dimensions:

(a) Rods 0.25 in diameter with lengths varying between 0.25 in and 3.0 in.

(b) Square bars, height and width 0.25 in with lengths varying between 0.25 in and 3.0 in.

The pyrocarbon specimens were discs with a diameter of about 0.25 in, and thickness ranging from 0.025 in to 0.003 in.

(5) To characterise the materials and as part of the post-irradiation work, the following properties were measured:

(a) Electrical resistivity at room temperature (four point method).

(b) Mean coefficient of linear thermal expansion 20-400°C (CTE) (silica dilatometer).

(c) Dynamic Young's modulus (resonating bar).

(d) Bulk density (from weight and macroscopic dimensions).

For the pyrocarbons in addition to (a) and (b) the following properties were measured:

(e) Density (sink-float method using methanol-bromoform mixtures).

(f) Crystallite height L_c (by X-ray diffraction from width of the 0002 reflection). This measurement was also made for some of the graphites.

(g) Distance between lattice planes (by X-ray diffraction from position of 0002 reflection).

(h) Bacon Anisotropy Factor (BAF) (by X-ray diffraction from the variation of intensity of the 0002 reflection with direction in the specimen).

(6) Dimensional changes were measured with:

(a) a travelling microscope, measuring between the end faces of the specimen (bulk synthetic graphites) or between fiducial holes (pyrocarbon discs)

(b) a linear displacement transducer using steel or silica standards.

Reproducibility of the length measurements varied from ±1 μm to ±5 μm depending on the quality of the specimen.

(7) Some properties of the bulk synthetic graphites are given in Table 1. Materials which have been of more special practical interest in the Dragon Reactor appear first in the list and are designated G00, G9, G5, HX30 and IG. Brief descriptions of these materials are given below.

G00 is British Pile Grade A graphite which has, however, received two pitch impregnations during its manufacture, rather than the single impregnation normally used for PGA. It is the graphite used as reflector in the Dragon Reactor.

G9 is a fine-grained extruded graphite, a derivative of Morganite Carbon EY 9. This material was purchased in the baked form, and was

Table 1

Properties of Bulk Synthetic Graphites

Dragon Material Designation or Number	Density g cm^{-3}	Mean CTE (1) 20–400°C 10^{-6}/°C		Electrical Resistivity (1) mΩ cm		L_c Å	Young's Modulus (1) 10^{10} dyne cm^{-2}	
		//	⊥	//	⊥		//	⊥
G00	1.78	1.3	3.2	0.57	0.87	680	13.3	6.0
G9	1.79	1.9	4.6	1.90	3.70		16.5	8.3
G5	1.74	1.5	3.5	0.90	1.50	380	11.2	6.2
HX30	1.80	1.3	2.9	0.73	1.30	560	13.4	6.4
IG	1.80	4.0	4.5	0.74	0.87	400	9.6	8.6
1	1.79	5.0	4.8	0.96	0.91	320	8.6	8.8
2	1.66	2.0	2.6	0.60	0.71	620	8.8	6.6
3	1.73	1.1	2.0	0.55	1.01	-	9.2	3.8
5	1.88	4.5	4.7	0.80	0.85	360	13.1	12.3
6	1.67	5.5	4.8	1.98	1.89	240	7.1	7.1
7	1.85	4.1	4.6	0.78	0.85	310	11.9	11.0
17	1.72	5.3	5.2	1.03	0.90	240	8.7	7.2
18	1.73	3.7	2.5	1.30	0.97	510	6.7	10.3
21	1.74	5.5	5.8	0.88	0.90	300	10.7	10.4
22	1.96	10.7	0.5	1.85	0.47	-	3.1	19.8
34	1.80	3.9	3.7	1.49	1.47	333	11.3	11.5
35	1.69	3.0	4.5	1.39	1.11	-	8.9	5.6
37	1.75	3.0	2.6	1.13	0.93	512	6.6	9.5
58 (2)	2.19	0.25	24.1	~0.1	very large	144	-	-
66	1.69	3.1	3.8	0.56	0.67	-	9.5	7.2
67	1.61	6.2	5.4	1.40	1.40	-	5.2	5.2
68	1.69	5.4	6.9	1.15	1.26	-	9.1	8.4
69	1.81	4.6	3.9	1.62	1.11	-	8.9	5.6
70	1.67	3.1	3.1	1.50	1.40	-	7.8	8.7

(1) Directions indicated are with respect to direction of forming except in the case of the bulk pyrolytic carbon (No. 58) in which // means the direction parallel to the substrate plane.

(2) Material 58 is bulk pyrolytic carbon deposited from methane at 2000°C. The Bacon Anisotropy Factor = 11.3

purified and graphitised at 2700°C by the Dragon Project. In contrast to G5 graphite which has no "non-graphitising" fillers, G9 is known to contain appreciable quantities of carbon black.

G5 is a fine-grained graphite developed by Compagnie Pechiney working under contract to the Dragon Project. The starting material for manufacture was reground French nuclear graphite of which about $\frac{1}{3}$ was micronised. For extrusion a conventional pitch binder was used and the material received a double pitch impregnation prior to graphitisation at 2700°C.

HX30 graphite is very similar in its manufacture to G5. The starting material was reground British Pile Grade A graphite but the grist size was rather coarser than in G5. A conventional pitch binder and impregnant was used. HX30 was developed by the Dragon Project collaborating with Chemical Engineering Division, AERE, Harwell.

More information about these materials is given in [7] and [8].

IG is an early version of an improved type of extruded reactor graphite designed for better dimensional stability under neutron irradiation. This material is similar in type to that discussed in [9].

In Fig. 3 photomicrographs are given illustrating the microstructure of various types of graphites:

Fig. 3a : a coarse-grained anisotropic graphite, e.g., GOO and type 3

Fig. 3b : a fine-grained anisotropic graphite, e.g., G5

Fig. 3c : an isotropic graphite containing spherical grist particles, e.g. 1G and types 1, 5 and 21

Fig. 3d : a very fine-grained isotropic graphite, e.g. types 34 and 35

The pyrocarbons were prepared by methane pyrolysis at temperatures between 1400°C and 2300°C in a fluidised bed using tantalum discs as substrate. The discs were stripped from this substrate prior to evaluation and irradiation. These materials were prepared as being representative of some of the pyrolytic carbons which may be deposited as fission product retaining barriers or spherical nuclear fuel particles. The pyrocarbons were supplied by Dr. C. Vivante of the Dragon Project. Deposition temperatures and properties are given in Table 2.

4. RESULTS

From the present experiment two types of results have been obtained. For a number of graphites, notably GOO, G5, G9, IG and the anisotropic pyrolytic graphite, as deposited at 2100°C (material 58), the dimensional changes as a function of neutron exposure have been measured over a dose range of

Table 2

Properties of Dragon Pyrocarbon Discs

No.	Deposition Temperature °C	Density g/cm^3	BAF	L_c Å	$\frac{c}{2}$ Å	ρ mΩ cm	$\bar{\alpha}_{20-800°C}$ 10^{-6} °C^{-1}
1	1500	1.42	1.21	20	3.451	5.61	
2	1600	1.60	1.25	68	3.408	2.81	
3	1700	1.64	1.15	67	3.407	4.03	4.14
4	1800	1.79	1.12	92	3.409	3.42	
5	1900	1.94	1.18	111	3.391	1.98	4.56
6	2000	2.08	1.25	128	3.389	1.34	
7	1500	1.55	1.11	48	3.404	5.17	
8	1600	1.61	1.36	75	3.401	2.41	
9	1700	1.56	1.13	62	3.401	7.29	
10	1800	1.68	1.17	74	3.404	3.36	
11	1900	1.80	1.10	85	3.393	3.75	4.38
12	2000	2.07	1.22	122	3.386	1.36	
13	1400	1.46	1.13	30	3.411	4.93	
14	1500	1.63	1.25	25	3.457	3.35	
15	1800	1.85	1.15	90	3.418	3.35	
16	1900	1.82	1.17	105	3.420	3.33	6.6
17	2000	1.99	1.11	110	3.406	2.24	6.2
21	1800	1.75	1.15	96	3.427	3.33	
22	1800	1.85	1.15	95	3.422		
23	1800	1.64	1.10	73	3.405	4.90	5.5
26	2000	2.07	1.21	126	3.398	1.53	5.9
27	2000	2.08	1.27	135	3.411	1.51	
28	2000	2.12	1.23	158	3.413	1.07	
29	2100	2.09	1.28	147	3.409	1.27	
31	2300	2.15	1.13	149	3.409	1.22	3.75

The X-ray measurements were performed by Euratom, Petten Establishment [25].

~25 x 10^{20} n cm^{-2}. These results are shown in Figs. 4, 5, 6, 7 and 8.

For a great many new graphites and pyrocarbons up till now only one data point at a fairly low dose, 2-4 x 10^{20} n cm^{-2} is available. Results for the bulk synthetic graphite are given as linear shrinkage rates in Table 3. Since at 600°C at these doses differences between graphites are rather small, the results are omitted. The results for the pyrocarbons are shown in Figs. 13 and 14.

The main points arising from these results are:

(1) In all the synthetic graphites irradiated, with the exception of the pyrolytic material (58) in the c-axis direction, a contraction is observed at all three temperatures. In some cases, mainly at 600°C this contraction is preceded by a very slight expansion.

(2) At any temperature in extruded graphites the contraction rate is larger in the parallel than in the perpendicular direction. The only exception is in G9 at 600°C and also at 900°C and 1200°C up to 3 x 10^{20} n cm^{-2}.

(3) In all graphites in any direction the contraction rate, at least at low dose, is largest at 1200°C and smallest at 600°C. This is illustrated in Fig. 9, showing the temperature dependence of the shrinkage rate of several graphites.

(4) Different graphites, although behaving in a similar way qualitatively, show quantitative differences in their dimensional changes. This is also well illustrated at low doses by Fig. 9. At some temperature there seems to be a rapid increase in contraction rate but this temperature lies higher for the graphites with the smallest contraction rates. For GOO and IG this point lies above 900°C, but for the rapidly shrinking materials like pyrocarbons 17 and 21 it may even be below 600°C. For intermediate cases like G5 and pyrocarbon 31 this temperature lies somewhere in-between 600°C and 900°C. A further striking demonstration is given by graphs showing the volume shrinkage as a function of neutron exposure for several graphites at the three temperatures (Figs. 10, 11 and 12). The order is the same at all temperatures.

(5) The contraction rates are not constant but they vary with neutron dose. The most pronounced effects are:

at 600°C : increase in contraction rate in both directions

at 900°C : increase in contraction rate in the direction parallel to extrusion, decrease in the perpendicular direction. Especially in G5 and G9 the perpendicular direction is beginning to expand. In G5 the minimum occurs at higher dose than in G9.

Table 3

Bulk Shrinkage Rates % per 10^{20} n cm^{-2} at 900°C and 1200°C

Material Designation or Number	Resistivity Index (1) $(2\rho_{\perp} + \rho_{//})$	Accommodation Factors $A_{//}$	$A_{\perp}$	Anisotropy $\frac{\alpha_{\perp}}{\alpha_{//}}$	$E_{\perp} + E_{//}$ 10^9 dyne cm^{-2}	Shrinkage Rate $\frac{\Delta L}{L_o}$ % per 10^{20} at 1200°C //	$\perp$	Shrinkage Rate $\frac{\Delta L}{L_o}$ % per 10^{20} at 900°C //	$\perp$	
Capsule V										
GOO	2.31	0.068	0.135	2.46	193	0.110	0.088	0.030		A Cubes, Rods 6-19 mm long ϕ 6.3 mm
G5	3.90	0.075	0.146	2.33	184	0.106	0.072	0.045		
G9	9.30	0.089	0.185	2.42	248	0.194	0.220	0.122		
IG	2.48	0.164	0.182	1.12	182	0.077	0.028			
1	2.83	0.199	0.192	1.04	174	0.064	0.066	0.018		
2	2.02	0.094	0.112	1.25	154	0.062	0.060	0.019	0.011	
3	2.57	0.062	0.093	1.78	130	0.040	0.020	0.014		
5	2.50	0.182	0.190	1.05	254	0.133	0.130	0.026	0.030	
6	5.87	0.218	0.194	1.14	142*	0.106	0.088	0.034	0.030	
17	2.96	0.210	0.207	1.02	159	0.065				
21	2.70	0.217	0.228	1.05	211	0.600	0.062			
35	3.70	0.129	0.183	1.50	145	0.032	0.014	0.006		
66	1.90	0.132	0.157	1.22	167	0.070	0.056	0.015	0.007	
68	3.67	0.212	0.267	1.28	175	0.086	0.054	0.020	0.022	
69	4.42	0.185	0.161	1.18	165	0.068	0.075			
70	4.76	0.132	0.130	1.02	181	0.136	0.127			
Capsules I-IV										
GOO	2.31	0.068	0.135	2.46	193	0.180	0.122			B Bars, Rods 76 mm long ϕ 6.3 mm
G5	3.90	0.075	0.146	2.33	184	0.280	0.200			
IG1	2.48	0.164	0.182	1.12	182	0.130	0.085			
35	3.70	0.129	0.183	1.50	145	0.086	0.114			
HX30	3.33	0.068	0.115	2.30	197	0.188	0.230			

* For category A these numbers are based on results from one specimen after 2-3 x 10^{20} n cm^{-2}

(1) See discussion of results

at 1200°C : contraction rate decreases in both directions in all materials. In G5 and G9 perpendicular a turnaround is again observed, again in G9 at lower dose than in G5.

(6) Contraction rates in pyrocarbon discs can be correlated to bulk density, (Figs. 13a, b and c) as well as to crystallite height (Figs. 14a, b and c), L_c. For pyrocarbons with the largest crystallite height and the highest density the smallest contraction rate is observed.

(7) The essential character of the dimensional changes occurring in the crystallites of all the materials is well illustrated by the very highly oriented pyrolytic carbon shown in Fig. 8, viz., crystallite expansion in the direction perpendicular to the basal planes and crystallite shrinkage in the basal plane direction; the initial rates of damage increase with temperature in the range 600–1200°C.

(8) Changes in electrical and thermal conductivity (not shown here) are smallest after irradiation at 1200°C and largest after irradiation at 600°C. Following a rapid initial decrease in conductivity the rate of change becomes much less. Changes in Young's modulus (not shown here) show a similar behaviour.

(9) The mean coefficient of linear thermal expansion 20–400°C changes little on irradiation. The increase rarely exceeds 20% of the pre-irradiation value. At doses around 10^{21} n cm^{-2} there is a decrease in some materials, (Figs. 15a, b, c).

5. DISCUSSION

5.1 Characterisation of Materials

From the description of the mechanism given in Section 2 it follows that several structural characteristics of a graphite should be important in determining the magnitude of the dimensional changes and therefore also the differences with other graphites. One of the aims of this investigation is to give criteria for the selection of the best possible graphite for a specific reactor purpose. Therefore it is desirable to arrive at a quantitative relationship between structural characteristics and neutron-induced dimensional changes. In the model described, two separate points of prime importance can be distinguished:

(a) the damage retained by the crystallite, and the attendant crystallite dimensional changes

(b) the extent to which the crystallite dimensional changes give rise to bulk dimensional changes, i.e., the degree of accommodation furnished by crack-closure and the ability of the crystallite to deform or creep under irradiation induced

stresses. This may become of overriding importance with increasing crystal strains.

Finally it must be remarked that, notably in the USA, the differences in behaviour between graphites have been related to differences in crystallinity and crystallite perfection. Particularly at high temperatures an appreciable part of the dimensional changes has been attributed to an atomic ordering process, or graphitisation, especially in the poorly graphitic regions of the material such as the binder [10]. This has been termed the Two Phase Model [11]. It seems rather difficult to rationalise results other than qualitatively in this way.

About the characterisation of a graphite in relation to points (a) and (b), the following may be said:

(a) In the temperature region in which vacancies become mobile two new processes determining the fate of a vacancy become competitive with the processes of vacancy-interstitial annihilation and formation of vacancy lines already existing at low temperatures. One is vacancy clustering, thought not to cause a large contraction in the a-axis direction but instead, by collapse of large clusters, causing some c-axis contraction. The other is trapping of the vacancies at grain boundaries and tilt boundaries, a process that is supposed to contribute considerably to a-axis contraction. The relative importance of the latter process should be very dependent on the time a wandering vacancy needs before it is trapped. This is determined by its mobility and the path length to be covered, and is therefore dependent on the temperature and crystallite diameter. This seemed to follow from early results [12] where a correlation of (crystallite) dimensional changes with electrical resistivity was observed. Since the predominant contribution to the electrical resistivity in polycrystalline graphites has been demonstrated to be grain boundary scattering, the electrical resistivity can be taken as a measure for the crystallite diameter, at least for not too different structures [13].

In the present work also, the electrical resistivity has been measured to obtain an easy comparison of crystallite diameters in synthetic graphites. The electrical resistivity index treats the electrical properties in a volumetric manner $\left(2\rho\perp + \rho//\right.$ to forming$\left.\right)$ in an attempt to allow for anisotropy. Differences in density, usually rather small, were not corrected for.

A second method is the measurement by X-ray diffraction of the crystallite size. In practice the effective crystallite diameter is unmeasurable and therefore the crystallite height L_c is used, assuming that L_c is a good measure for L_a. This is not entirely without doubt since probably the temperature regions for c-axis and a-axis crystal growth are not identical [14].

A correlation between L_c and the electrical resistivity index of several bulk synthetic graphites is shown in Fig. 16. For the pyrocarbons alone the correlation is shown in Fig. 17. Although there is a good correlation between these properties, for a special group of graphites, notably graphites made of spherical grist particles, there is a deviation. It is not immediately clear what the reason is.

Also, although in the conventional synthetic graphites the correlation between L_c and resistivity is reasonably close, as a group the pyrocarbon discs behave differently from the bulk synthetic graphites. Here the differences in density are much larger, 1.50-2.10 g cm^3, so that a correction for density should be applied.

The discs with density about equal to that of the bulk graphites do fall on or near the line, but this is perhaps fortuitous because the effect of a lower density on the resistivity will be strongly dependent on orientation, shape and distribution of the pores. On the whole for the pyrocarbons, L_c may be a better criterion although little is known with certainty about the shape of the particles. In particular one has the feeling that in the carbons with the highest density, where during manufacture a marked polymerisation in the gas-phase has taken place, one may be underestimating L_a. For the present it can be said that the good correlation between L_c and resistivity index for a number of polycrystalline graphites gives some confidence in their use as a measure of crystallite diameter and thus as a first measure of the likely crystallite dimensional changes of new graphites. However the deviation of other groups, notably the spherical grist and gilsocoke graphites shows that one has to be extremely cautious in using these criteria.

For very anisotropic materials the resistivity index is meaningless. Here L_c must be relied upon.

(b) In the model originally developed by Simmons [15] the parameter A_x determines the extent to which crystallite dimensional changes are transmitted as bulk changes. A_x essentially is a measure of the distribution of an applied load in the direction x between the c-axis and a-axis crystal direction in the aggregate. In the original form A_x was shown to be the same for thermal strains and radiation induced strains and so the magnitude of A_x could be found from measurement of linear thermal expansion coefficient, (CTE).

It became apparent however, that the relation between dimensional changes and CTE breaks down at high doses [5] and it was even suggested [3] that it may only apply to certain structures such as PGA-like materials at small crystal strains.

For well graphitised graphites A-factors as a function of crystal strain have been measured by bromination but also here the results become questionable at high crystal strains [16].

As a quantitative guide for PGA-like structures at low neutron doses, for selection purposes for instance, the CTE is regarded as a good guide for estimating bulk dimensional changes for graphites with similar crystal size.

In this report it is assumed in the first instance that also for graphites with different structures, such as the isotropic graphites and the pyrocarbons, the CTE does give a good indication of the presence and relative importance of Mrozowski cracks in which the c-axis expansion is accommodated, so that initial contraction rates for a given crystallite size (see (a)) may be estimated from the magnitude of the CTE, and also perhaps the turnaround dose, where the contraction in the perpendicular direction changes to an expansion. Strictly speaking the thermal expansion coefficient $\frac{1}{L}\frac{dL}{dT}$ must be measured at the irradiation temperature. A-factors may be temperature dependent and thus different A-factors apply to 1200°C and 600°C. Mainly for practical reasons the mean value over a not too large temperature region has been taken here and A-factors obtained so are accurate enough to serve as a rough guide.

The possible influence of creep is as yet a less tangible factor. It seems safe to assume that, when stressed under and particularly as a result of irradiation, crystallites will tend to deform in essentially the same way as when stressed out of pile, that is by C-44 shear, and possibly by twinning. Thus one should expect that the Young's modulus of a material gives a first indication of whether a material is likely to be able to accommodate large crystal strains by plastic deformation. Indeed it has been shown that the creep constant is dependent on the initial modulus. High elastic strain potential measured prior to irradiation indicates that plastic deformation under irradiation will be facilitated [17]. A qualitative illustration of this effect has been observed in subsidiary experiments. Thus a piece of a fine grained anisotropic pyrolytic graphite, expanding in the c-axis direction during irradiation, fractured its thick walled graphite container and thus apparently showed little tendency for creep. Judging by the difficulty to shear (tear??) off layers for electron-microscopic preparations the material had a high C-44. On the other hand graphite 22, an anisotropic well crystallised

graphite formed by hot pressing at graphitising temperatures and possessing an anomalously low Young's modulus, showed behaviour which suggested a very large radiation creep.

Evidence from the present work that irradiation creep is important in suppressing crystallite dimensional changes even at low doses is discussed later.

Summarising this discussion, it appears that for optimum dimensional stability under irradiation the necessary characteristics are:

1. A large crystallite diameter. In terms of measurable properties this means a large L_c or a low electrical resistivity. For certain groups these criteria may not be exact but they probably serve as a general guide.

2. For any given crystallite dimensional change rate the graphite (and the direction in the graphite) having the CTE nearest to $\frac{a_c + 2a}{3} \simeq 9 \times 10^{-6}\ ^{o}C^{-1}$ suffers the smallest bulk dimensional changes. In most cases (with the exception of very anisotropic graphites such as the hot pressed graphite (22) and the bulk pyrolytic carbon (58)) the CTE is much lower than $9 \times 10^{-6}\ ^{o}C^{-1}$ which implies that if the crystallite volume remains constant, a shrinkage will always be observed, being smallest for the highest CTE. (If the crystallite volume increases then even with CTE below $9 \times 10^{-6}\ ^{o}C^{-1}$ an expansion could in principle be found.)

   On the other hand for a high CTE the dose at which contraction ceases and expansion begins is probably reached at lower dose. This expansion may well prove to be the prime nuisance in the use of graphite at high irradiation doses. This again stressses the importance of small crystallite dimensional changes.

3. If the crystal deforms easily by shear, crystallite dimensional changes may be effectively diminished. A crystal volume change would remain unchanged however, as shear carries no volume effect.

4. In all cases isotropy is a necessary prerequisite for good stability.

5.2 Analysis of Irradiation Results

5.2.1 Bulk Synthetic Graphites

To examine these points using the experimental evidence, the apparent crystallite dimensional changes have been first calculated in GOO, G5, G9, IG and the bulk pyrolytic carbon (58). These

have been calculated from the bulk dimensional change at small increments of dose and the measured CTE's using formulae 1 and 2, Section 2.4. Results are shown in Figs. 18, 19 and 20. It must be remarked that this analysis becomes increasingly prone to very large errors as isotropy is approached: indeed the crystallite dimensional changes for fully isotropic materials cannot of course be determined from equations (1) and (2). For all isotropic graphites and pyrocarbon and for materials on which data is incomplete, this problem is overcome by assuming no change is occurring in the crystallite volume, i.e., $A_x = 0.33$ gives $\frac{1}{L}\frac{dL}{dN} = 0$. A consideration of Fig. 1 suggests that for temperatures above 600°C this is a reasonable first approximation.

Figs. 18, 19 and 20 show that the relative magnitude of the crystallite changes for graphites with different crystallite sizes is generally consistent with the proposed mechanism.

Thus for a given material the crystallite dimensional change increases when the irradiation temperature is raised from 600°C through 900°C to 1200°C. This is identified with the increasing vacancy mobility leading to enhanced vacancy loss at boundaries as previously discussed. The degree of enhancement of crystallite dimensional instability does not change in the same way with temperature for all the materials. A "breakaway" temperature above 900°C seems to be indicated for the G00 graphite whilst for the pyrolytic carbon the break is not so sharp and appears to be between 600°C and 900°C. This is consistent with the influence which the crystallite size would be expected to have on the rate of loss of vacancies, i.e., the loss-rate increases sharply at a lower temperature for the material with the smaller crystallites (pyrolytic carbon 150Å) than for the graphite with the larger crystallites (G00 700Å). Features of these graphs describing "two phase" effects found in G9 graphite will be discussed later.

In Fig. 21, the temperature and dose dependence of the crystallite dimensional changes calculated for the G00 graphite are shown.

A word of caution must be introduced here as to what weight we attach to the actual value of these changes, the c-axis changes in particular. Consideration of formula (1) shows that the very small A-factors of most graphites act as an attenuator for c-axis crystal strains. But when we work round the other way as we do when we calculate $\frac{\Delta X_c}{X_c}$ from $\frac{\Delta L}{L}$ the same A-factor becomes a very large lever. Small uncertainties in the A-factors and in $\frac{\Delta L}{L}$, which are unavoidable because for the two directions two different specimens are used, cause very large uncertainties in $\frac{\Delta X_c}{X_c}$. It

would be wrong, for instance, to calculate from these graphs what the crystallite volume changes are. Probably all that can be said is that no volume contraction is observed and that volume increases are probably very small, especially at 600°C. Actual crystallite volume changes are most important since they determine the high dose behaviour and probably the behaviour of isotropic high CTE graphite.

Concerning the dose dependence shown in these graphs, it should be remarked that it has been shown that the accommodation factor effective during irradiation cannot be determined by CTE measurements after large crystallite strains, say in excess of 15% even for PGA graphite. In fact A probably increases much more than the CTE indicates so that in our graphs $\frac{\Delta X_a}{X_a}$ and $\frac{\Delta X_c}{X_c}$ are almost certainly overestimated at high dose. The qualitative aspects are presumably correct. At 600°C and 900°C the crystallite dimensional change rates increase with dose whereas for GOO graphite at 1200°C they decrease. The acceleration in rate may be connected with the formation and collapse of vacancy lines: in GOO graphite at 1200°C vacancy line formation may be suppressed relative to clustering. These clusters would collapse in the c-axis direction giving a diminished c-axis expansion coupled with a lower a-axis shrinkage.

The uncertainties and difficulties occurring at high temperatures of irradiation as a result of the effects of crystallite size considerably increase the problems of quantitative correlation and prediction of behaviour. Furthermore there are now indications that internal mechanical effects in the material can play a significant role in the dimensional changes at much lower doses than thought previously.

The first indications of this were obtained from attempts to relate the crystallite dimensional change rates observed at 1200°C to material properties. By assuming a constant volume state in the crystallites the basal plane shrinkage rates were determined for several materials irradiated in the form of rods in capsule experiments I-IV (see Table 3). These results are shown graphically in Figs. 22a and 22b. The latter figure could be interpreted as indicating that an estimate of the initial rate of dimensional change in a new graphite might be possible from a knowledge of the electrical resistivity (to yield the crystallite dimensional changes) and the coefficient of thermal expansions (to translate to the bulk). However, it should be noted that material 35 exhibits much smaller dimensional changes than expected on these grounds. It is noteworthy that Young's modulus of this material is rather below that of the other graphites in this group. This may be a case therefore where the dimensional changes are modified by irradiation creep.

In the fifth capsule a number of new graphites were irradiated in the form of cubes or short rods, (see Table 3). These specimens

received a dose ranging between 2 and 4 x 10^{20} n cm^{-2}. In addition the reactor power was 50% higher than for previous irradiation and the geometry of the capsule environment was somewhat altered. Until the effects of these changes on the neutron spectrum have been allowed for it is not possible to relate these results quantitatively with those obtained previously. However, specimens of the older graphites were also included and the results shown in Table 3 suggest that the new spectrum is rather less damaging.

However, it is still worthwhile to take these results as a group in themselves and examine whether the correlation indicated in Fig. 22b holds true. The computed crystallite shrinkage in the a-direction is plotted as a function of the electrical properties in Fig. 23. This clearly shows that taken as a whole, there is no correlation between these two parameters. A reasonable correlation is found if one restricts attention to the materials with $(E_{//} + E_{\perp})$ between 150 and 190 x 10^{9} dyne cm^{-2}. It is notable that materials 3 and 35 both having a relatively low Young's modulus exhibit much lower dimensional changes than one would predict from their electrical resistivity and thermal expansion. On the other hand materials 5 and 21 show large shrinkages, unexpected from their relatively low electrical resistivity and high thermal expansion. Both these materials possess an unusually high Young's modulus.

These results strongly indicate that the dimensional changes suffered during irradiation even at low doses can be very significantly modified by internal mechanical effects. In particular the greater the elasticity of the unirradiated graphite (the lower Young's modulus) the more the crystallite dimensional changes are diminished by irradiation creep.

5.2.2 Pyrocarbons

For the pyrocarbons the data are still less complete since shrinkage in one direction only has been measured. In addition for most of the specimens CTE could not be measured due to technical difficulties connected with the small specimen size.

Since the pyrocarbons investigated here are all rather isotropic it seems reasonable to assume, until further data on the density change are available, that also in the direction perpendicular to the plane of the disc a shrinkage takes place, up to 25% less than in the plane, depending on the Bacon Anisotropy Factor.

This appears to be in contradiction with the results of Bokros and Price [18], who, for specimens of comparable anisotropy, report expansions perpendicular to the disc plane, at least at 900°C and 1200°C. The difference is, however, that their data refer to one point at a fairly high dose, about 2.3 x 10^{21} n cm^{-2}. At these doses, especially for these small crystallite sizes, one

would expect that perpendicular contraction has turned into an expansion, as has been observed for many bulk synthetic graphites. In their analysis Bokros and Price do not consider an effect like this. Furthermore they assume that no cracks suitable for accommodation of c-axis strains are present. This leads them to the conclusion that one of the main mechanisms responsible for dimensional changes in the pyrocarbons is an atomic densification, [19] the fact that the densification is proportional to the initial density defect being quoted to support this [20].

However, the present measurements of CTE on several of the discs indicate the presence of Mrozowski cracks to approximately the same extent as in bulk synthetic graphite, and furthermore it is shown that no obvious relation exists between CTE and density. In fact the lowest CTE is found in the specimen with the highest density. This is not altogether unexpected since this disc was deposited at the highest temperature, 2300°C, so that cooling stresses have been most severe here.

There seems to be no sound a priori reasons to regard the pyrocarbons as a group of materials differing fundamentally from bulk synthetic graphites. Indeed on an atomic scale there is little difference in the environment of the carbon atoms. In both cases the carbon atoms find themselves arranged in layers in quite the same way, forming graphite crystallites. Seen at this level the main points of difference between different carbons and graphites lie in the regularity of the stacking of the layer planes forming the crystallite, the distance between the layer planes and their perfection, and the size of the crystallites. Large differences between different graphites and carbons exist in the way these crystallites are packed to form solid, polycrystalline bodies. These differences arise mainly from differences in the manufacturing process, including heat treatments, and they manifest themselves in the structure as differences in porosity, orientation of the crystallites, presence and extent of Mrozowoki cracks, etc. Pyrocarbons as a group distinguish themselves from other graphites by their small crystallite size and the absence of large pores. A large variation is possible in degree of preferred orientation of the crystallites, density and crystallite size.

Ideally it should be possible to interpret the irradiation effects in pyrocarbons in the same way as for bulk synthetic graphites and to explain differences in behaviour in terms of differences in structure.

If we do this it becomes rather hard to understand why shrinkage rates are correlated with density as shown in Fig. 13 since the density defect does not appear to be a measure for the importance of the Mrozowski cracks. It is therefore postulated that the shrinkage rate is in actual fact correlated with crystallite size: the correlation with density is only apparent and is a result of the close correlation of density and crystallite size in this group of pyrocarbons.

For the discs for which CTE has been measured, and thus A-factors are known, crystallite dimensional changes have been derived, assuming again no crystallite volume changes. The result is given in Table 4 and shown in Fig. 24 versus electrical resistivity. Even below 100Å the crystallite size is seen to be a factor of importance for the crystallite dimensional change rates.

5.2.3 Two-phase Effects in G9 Graphite

Up to this point results have been treated for all materials alike under the assumption that the main mechanism responsible for the observed bulk dimensional changes is in the crystallite dimensional changes. It is possible that other mechanisms may contribute, especially in other than the classical, well graphitised graphites. These mechanisms if present may mask to some extent the quantitative relationship in the Simmons-Reynolds theory. It is conceivable that effects due to unrelieved cooling stresses or the presence of very disordered graphite are responsible for part of the deviations of actual behaviour from that expected.

In one case in the present work strong evidence exists for the presence of a second mechanism, that is in G9.

Although the general behaviour of G9 is consistent with the model outlined if one takes into account the fact that it contains extremely fine-crystalline material (carbon black) it nevertheless shows some anomalous behaviour when looked at in detail, (Fig. 5).

At 600°C the contaction is anomalously large from the outset, and it does not show any sign of initial expansion. Moreover, it shrinks more rapidly in the transvere direction than in the parallel direction at 600°C, which is unprecedented. At 900°C and 1200°C it behaves as an isotropic graphite in the early stages of irradiation, though its physical properties clearly indicate that it is not at all an isotropic material. At higher doses the contraction rate in the transverse direction begins to decrease. It was suggested in [12] that the numerical relationships of the Simmons-Reynolds theory was masked in G9 by the existence of a second process tentatively identified with radiation-induced relief of frozen-in microstresses. These microstresses, generated on cooling down from graphitising temperature as a result of the large difference in thermal expansion in the a- and c-direction, are in G9 probably not relieved by opening up of Mrozowski cracks or plastic deformation to the same extent as in well-graphitised materials. This is due to the small crystallite size and heavy cross-linking. These stresses act as a compression in the c-axis direction and for extruded graphites they will therefore be larger in the transverse than in the parallel direction. The radiation-induced relief of these stresses can be seen as a yielding of the structure under these stresses, and should therefore give a length change larger in the transverse than in the parallel

Table 4

a-axis Crystallite Shrinkage Rate for some Dragon Pyrocarbons

No.	A-factor	L_c Å	Resistivity Index mΩ cm	g_a % per 10^{20} n cm^{-2} 900°C	1200°C
3	0.168	67	12.09	-1.15	-1.52
5	0.183	111	5.94	-0.47	-0.84
11	0.176	85	11.25	-0.72	-1.32
16	0.256	105	10.00	-1.57	-1.85
17	0.240	110	6.72	-0.86	-1.23
23	0.216	73	14.70		-3.34
26	0.230	126	4.59	-0.29	-0.68
31	0.154	149	3.66	-0.11	-0.37
For comparison					
G00			2.31	-0.06	-0.22
G5			3.90	-0.15	-0.36
IG			2.48	-0.08	-0.22

$g_a = \frac{1}{X_a}\frac{dX_a}{dY}$ was calculated assuming crystallite volume changes are zero.

direction.

An alternative hypothesis is that the isotropic contraction is caused by the rapid shrinkage of the carbon black. This will also lead to the stressing of the matrix graphite and a corresponding relief of the stresses by irradiation creep as described above.

At 600°C applying the Simmons-Reynolds theory, one would expect a behaviour similar to that of G5. In fact a rather large contraction is observed for both directions. The extra contraction observed may be attributed to a second process, in [12] tentatively attributed to a stress relaxation.

Values of this stress relaxation can now be obtained at 600°C as the difference between the shrinkage observed at 600°C for G9 and that expected for G9 on the basis of G5 crystallite dimensional changes and A-factors for G9. To a first approximation it is assumed that this stress relaxation shrinkage is the same at all temperatures.

If a method could be found for estimating the shrinkage occurring in G9 at other temperatures in the absence of stress relief it would be possible to predict the initial shrinkage behaviour by adding the stress relief components given by the above. It is not possible to estimate the stress-free behaviour for temperatures above 600°C using the Simmons-Reynolds equations and the crystallite damage rates for PGA because of the interference from crystallite size effects in G9. It can be shown, however, that to a first approximation the behaviour of G5 graphite does indicate the stress-free behaviour of G9. The basis for this statement is the comparison of the apparent crystallite dimensional changes for these materials. Thus in Fig. 25 the crystallite dimensional changes are plotted as a function of dose at 900°C. These were computed from the coefficients of linear expansion and the bulk dimensional changes using the Simmons-Reynolds relationship. Inspection of Fig. 25 shows that for G5 the behaviour is normal: crystallite expansion in the c-direction and contraction in the a-direction. On the other hand, c-direction effects in G9 are anomalous. Up to a dose of about 3×10^{20} nvt an apparent c-axis shrinkage occurs but this is followed by the normal expansion at higher doses. This is now taken as indicating that the normal crystallite behaviour is masked at low doses by another process involving stress relief. The fact that following the initial stress relief period the rates of crystallite dimensional changes for G5 and G9 are almost identical, may be interpreted as showing that the dimensional behaviour of G5 approximates closely to that of "stress free" G9. It may also be noted that during the interval in which the stress relief effect is occurring in G9, only the c-direction crystal changes are anomalous. This suggests that the stress relief mechanism is associated with collapse in the c-direction or shear in the basal planes which would explain why the contraction associated with the relaxation is greater in the direction transverse to extrusion.

Having established that the behaviour of G5 should approximate to that of G9 when the latter material is stress-free, it is now possible to examine whether the shrinkage of G9 actually observed may be estimated by adding the stress relaxation component of shrinkage to that attributable to the normal mechanism. The result for 900°C and 1200°C is shown in Figs. 26 and 27 as fully drawn lines, together with the experimental points. Compounding the shrinkage in this way given a good measure of agreement with the contractions experimentally observed in G9. Especially the peculiar behaviour at low dose is reasonably well explained.

At higher dose there is a deviation. There may be several reasons for this. At 600°C there are still no signs that the second mechanism is exhausted, which probably should be the case if it were a stress relief mechanism. It may have been the case at 900°C and 1200°C so that the deviation starts where the second mechanism stops operating. A second possibility is that the actual behaviour of the hypothetical stress-free G9 would be different from that expected on the basis of G5 data, for instance on account of the still smaller crystallite size. If we follow this latter approach we can try to find out the behaviour of stress-free G9 by calculating the difference between the stress relaxation shrinkage found at 600°C and the actually observed behaviour at 900°C and 1200°C. The result is shown in Fig. 28.

The behaviour shown resembles very much that of G5, the main difference being slightly higher contraction rates and a turnaround at a lower dose. Both features are in agreement with the expectations for a graphite with a smaller crystallite size and a higher CTE.

It could also be argued that the reason for the deviation at high temperatures is that the assumption of a constant rate of stress relaxation for all temperatures is not correct. Creep experiments on this material have in fact shown a strong temperature dependence of irradiation creep in the temperature range 900-1200°C [1].

The case of G9, just described, is probably rare insofar as the contribution of this second mechanism is so large that the overall behaviour becomes clearly anomalous. The general conclusion is that in unorthodox materials, especially those containing appreciable amounts of less well graphitisable components, one should expect larger contraction rate than can be expected on the basis of the Simmons-Reynolds theory.

6. SUMMARY AND CONCLUSIONS

A wide range of graphitic materials have been examined in this work. The dimensional behaviour during irradiation in the temperature range 600-1200°C is complex but it is possible to draw some general conclusions.

(1) Although there is evidence that the number of point defects affecting properties such as thermal conductivity diminish with increasing temperature of irradiation, there is still a considerable shape change in the crystallites as a result of the agglomeration of the interstitials and vacancies produced.

(2) The rate at which the crystallites change shape (and hence the bulk dimensional instability) increases with irradiation temperature. However, for any given material there is a "breakaway" temperature above which the rate of dimensional change undergoes a much more rapid increase.

(3) For the most stable materials the breakaway temperature is above 900°C. On the other hand the least stable materials have a "breakaway" temperature below 600°C.

(4) The most important property dictating the "breakaway" temperature is the crystallite size. This is interpreted as showing that the rapid increase in rate of dimensional change is due to the increased loss of vacancies at crystallite boundaries.

(5) In addition to the crystallite size two other factors are of importance when the dimensional changes in different materials are quantitatively examined: these are the coefficient of thermal expansion and the initial value of Young's modulus.

(6) The correlation with the coefficient of thermal expansion is a natural extension of the existing theory for low temperature irradiation damage. However, dimensional changes even at low doses appear to be much larger than expected when the intitial Young's modulus is high and much lower than expected when Young's modulus is low. This is taken as clear evidence that crystallite shape change produced by irradiation is modified by deformation caused by stresses developed as a result of the mutual restrains between crystallites. Indeed there is some evidence that the Young's modulus is much more important in dictating the dimensional behaviour than is the coefficient of expansion.

(7) The mode of accommodation of crystallite (and bulk) dimensional change is tentatively identified with basal plane shear in the graphite crystallite activated by irradiation (irradiation creep). Materials of low modulus are capable of a greater shear resulting in a relaxation process which reduces both the c-axis growth and the a-axis shrinkage in the crystallites.

(8) Materials should be essentially "homogeneous". The mixing of grossly different grists or possibly the addition through impregnation of large fractions of non-graphitising components is likely to lead to dimensional behaviour which is not predictable from the material properties.

7. SPECIFICATION AND BEHAVIOUR OF GRAPHITE IN HIGH TEMPERATURE REACTORS

7.1 Environment

To place the discussion of the graphite requirements and behaviour in the correct context it is first worthwhile to mention briefly the

operating conditions of HTR's. The graphite environment in terms of the temperature of operation and total dose is conveniently divided into two parts.

(a) The structural graphite of the fuel elements in a reactor utilising a low enriched fuel cycle would be expected to be required to operate at relatively high temperatures, say 900°C to 1200°C, carrying a relatively high heat flux across the fuel container walls. Assuming an enrichment of 3% in the fuel and a fuel element pitch similar to that used in AGR, estimates indicate that in a power reactor with a 6 MW/m^3 (average) power density a peak dose of approximately 1.5×10^{21} n cm^{-2} (DIDO equivalent) would be accumulated in one year (75% load factor). At the present, residence times of between 1.5 and 2.5 years are contemplated. These figures would be a rough guide to a feed element in a feed breed reactor though further detailed calculation is required for this case.

(b) There is considerable freedom of choice for the temperature of operation of the moderator portion of the core of a low-enriched reactor core design. The peak dose would occur at the wall of the fuel element channel and would also be about 1.5×10^{21} n cm^{-2} (DIDO equivalent) in one year. In the case considered above with a fuel element pitch of about 44 cm (fuel channel radius ca. 13 cm), changes in the flux and spectrum lead to the integrated dose falling by a factor of approximately two for a position midway between fuel elements.

For reductions in power density with no major alteration in design these figures would be reduced pro-rata.

7.2 Specification and Behaviour

The minimisation of the rate at which the dimensions of a graphite change and the total amount of dimensional change are important for a number of reasons. Due to unavoidable temperature and flux gradients differential effects can occur which cause the generation of stresses as different parts of the same member attempt to deform at different rates. Thermal gradients can be minimised to some extent by choosing materials with good thermal conductivity. Thermal gradients are of special concern in HTR fuel elements since the structure must not only maintain its integrity in the face of differential stressing caused by irradiation induced dimensional changes, but it must also withstand thermal stresses arising from the relatively high heat fluxes in the fuel element wall. Thus properties affecting thermal stress should not be ignored in specifying the material. On the other hand it would be very costly to produce and test different materials for the fuel element and the rest of the core and if possible the same material should be used for both purposes.

A consideration of the results of the present work indicate that the following properties are important.

(i) Isotropy (as measured by CTE and Young's modulus)

(ii) Degree of crystallinity (electrical resistivity)

(iii) Coefficient of thermal expansion (CTE)

(iv) Young's modulus

(v) Ultimate tensile strength.

To act as a guide to the level of these various properties, Table 5 is given.

Isotropy is defined in terms of the ratio both of the coefficients of expansion and Young's modulii when specimens are cut parallel and perpendicular to the direction of forming. If the material is not isotropic in both these properties the dimensional behaviour will become grossly anisotropic especially at high doses. It is of greater importance that the material be isotropic in the case of the long-life moderator or breed block structure than for low-enriched or feed fuel elements as the doses in the former case will be very high.

The low electrical resistivity specified will result in a breakaway temperature which will be above 900°C. Also the temperature dependence of the shrinkage above 900°C will be lower than in the case of materials with a higher electrical resistivity. This gives freedom to fix the moderator temperature at a high level but it must be kept below 900°C for prolonged life. At the same time the minimisation of the temperature dependent shrinkage above 900°C reduces differential shrinkage stresses in the fuel element structures. A low electrical resistivity also indicates a high thermal conductivity leading to lower thermal stresses.

The coefficient of expansion might still play a part in dictating the initial rate of dimensional change and the ultimate shrinkage. However the present work has shown that this property should not be viewed in isolation: the initial rate of shrinkage can also be affected by Young's modulus and it is not unlikely that the shrinkage limit will also tend to be dependent on this property. There may be some incentive to move to materials with lower CTE's because of the adverse effect on thermal stresses of a high CTE. Low CTE materials may also be favoured for high dose intermediate temperature conditions to delay expansion effects.

The initial value of Young's modulus may be much more important in dictating graphite dimensional behaviour under irradiation than previously thought. Low values of this property indicate easy shear of the crystallites under irradiation which minimises the bulk dimensional change. Similarly the irradiation induced creep properties in the bulk material are improved when the initial value of Young's modulus is low and hence differential stresses are more readily relaxed. Finally, thermally induced stresses are minimised when the Young's modulus is low.

7.3 Dimensional Changes at High Doses

The doses to which fuel elements will be exposed in reactors using a low enriched fuel cycle will be relatively low; generally less than 4×10^{21} n cm^{-2} DIDO equivalent. Doses of this order would also apply

Table 5

Guide to Properties of a Graphite of Good Stability at High Temperatures of Irradiation

Isotropy (1)		<1.05
Electrical resistivity (milliohm cm)		preferably <0.8 but certainly less than 1.0
Coefficient of Thermal expansion (20-400°C) (2)		5×10^{-6} per °C
Young's modulus	(psi)	$1.0 - 1.2 \times 10^{6}$
	(dyne cm^{-2})	$6.9 - 8.3 \times 10^{10}$
Ultimate tensile strength	(psi)	>3,000
	(dyne cm^{-2})	$>20.7 \times 10^{7}$

(1) Isotropy is required from two viewpoints:

(a) the ratio of the CTE's in various directions with respect to the forming direction

(b) the ratio of Young's modulii in the same directions.

(2) Lower values may be acceptable, see text.

to feed fuel elements. There is little difficulty in achieving these doses at high temperatures to provide design data. Difficulties do arise, however, in the testing and provision of data for moderator blocks and breed elements in power reactors. In such cases the peak accumulated dose is such that for a 30 year life the material would have to withstand a total dose of about 4.5×10^{22} n cm^{-2} in a 6 MW/m^3 core or 3×10^{22} in a 4 MW/m^3 core, at a temperature below 800°C depending on the design.

Present evidence concerning the behaviour of graphite at high doses is very limited and restricted to low equivalent temperatures* [5, 21]. Furthermore to accumulate very high doses in a reasonable time the irradiation experiments have been carried out in the Dounreay Fast Reactor. Some difficulties may arise in interpreting these results because of dose-rate effects [2] but the general feature on irradiating at temperatures between 380°C and 750°C in DFR* for materials with properties similar to those in Table 4 is that up to a dose of about 1.5×10^{22} n cm^{-2} (DIDO equivalent) a shrinkage of about 3% is observed. At this dose the shrinkage appears to be saturating at least for the conditions studied. However, a number of considerations lead one to believe that maintenance of complete stability at high doses is unlikely although this was indicated previously [22] since it was assumed that at high crystal strains the crystallites would change shape at constant volume [23]. It is now thought that complete stability would only apply under the following circumstances.

(1) The material is completely isotropic in its Young's modulus (and CTE).

(2) The crystals are changing shape at constant volume.

(3) The grist particles are essentially spherical.

If the material is not isotropic, directions in which the c-axis of the crystals predominates will grow and shrinkage will occur in directions in which the a-axis is preferentially oriented. In such materials porosity is generated which could lead to loss of mechanical properties [5, 24].

Even when the material exhibits complete isotropy and the crystals are changing shape at constant volume it is difficult to conceive a mechanism which allows no volume change in the bulk material other than of the particles are spherical.

Thus it is now considered that the general effect which may be observed at very high irradiation doses is one of expansion due to either a volume expansion in the crystal or to the generation of porosity.

Until more data is available it would seem imprudent to design high power density HTGCR's with moderator structures which cannot, at least in part, be removed.

---

*Due to the dose-rate effect mentioned these would be expected to be equivalent to different temperatures in a HTGCR environment. The actual conversion to reactor equivalent temperature is not yet possible.

8. NOTE ADDED IN PROOF

The indications that the initial dimensional changes under irradiation at high temperature are related to Young's modulus have been strongly reinforced by experiments carried out in the Dragon Reactor [26]. The analysis clarifies relationships between crystallite shape, Young's modulus and the coefficient of thermal expansion and shows that the initial shrinkage rate may be correlated with crystallite shape and the bulk Young's modulus rather than the expansion coefficient.

9. REFERENCES

[1] R. Blackstone, L. W. Graham and E. H. Voice, "The Irradiation of Graphite in HFR - Petten", D.P. Report 555 to be published.

[2] General Reference: J. H. W. Simmons, "Radiation Damage in Graphite", Pergamon Press 1965.

[3] General Reference: W. N. Reynolds, "Radiation Damage in Graphite", pp.121-196 of Chemistry and Physics of Carbon. Edited by P. L. Walker Jr., Marcel Dekker Inc.

[4] B. T. Kelly, "Society for Chemical Industry", Second Industrial Carbon and Graphite Conference, April 1965, London, to be published.

[5] A. J. Perks and J. H. W. Simmons, Carbon 4 85 (1966).

[6] D. L. Reed, D.P. Report 559, to be published.

[7] L. W. Graham and M. S. T. Price, "The Fuel Element Graphite", D.P. Report 146.

[8] L. W. Graham and M. S. T. Price, "The Use of Carbon and Graphite in the Dragon Reactor Experiment", Soc. for Chem. Ind. Second Conference on Carbon and Graphite, April, 1965, London.

[9] J. M. Hutchion and R. P. Thorne, Soc. for Chem. Ind. Second Conference on Carbon and Graphite, April, 1965, London.

[10] D. R. de Halas and H. H. Yoshikawa, Proc. 5th Conf. Carbon (1961), Vol. 1 249.

H. H. Yoshikawa, et al., "Radiation Damage in Reactor Materials", IAEA, Vienna, 1963 p.581.

[11] W. C. Morgan, Carbon 4 215 (1966).

[12] R. Blackstone, P. F. Sens, L. W. Graham and E. H. Voice, "Experiments on the Irradiation of Graphite at High Temperatures", D.P. Report 351.

[13] J. C. Bowman, J. A. Krumhansl and J. R. Meers, Industrial Carbon and Graphite, London, 1957, p.52.

[14] J. Maire and J. Mering, Proc. 4th Conf. Carbon (1959), p.345.

[15] J. H. W. Simmons, Proc. 3rd Conf. Carbon (1957), p.559.

[16] J. E. Brocklehurst and J. C. Weeks, J. Nuclear Mat. (1963).

[17] B. S. Gray, J. E. Brocklehurst and A. A. McFarlane, Carbon 5 173, 1967.

[18] J. C. Bokros and R. J. Price, Carbon 4 441 (1966).

[19] J. C. Bokros and R. J. Price, Private Communication.

[20] J. C. Bokros and A. S. Schwartz, Private Communication.

[21] P. T. Nettley and W. H. Martin, Paper presented AIME Meeting, "High Temperature Nuclear Fuels", Delavan Wisconsin, October, 1966.

[22] R. A. U. Huddle, J. F. G. Condé and L. W. Graham, Brit. Nuc. Energy Soc. 5 345.

[23] B. T. Kelly, W. H. Martin and P. T. Nettley, Phil. Trans. Roy. Soc., London A.260 51 (1966).

[24] J. W. Helm, Carbon 3 493 (1966).

[25] G. Pellegrini, Euratom Petten, Private Communication.

[26] D.P. Report 556 - Parts I and II (to be published).

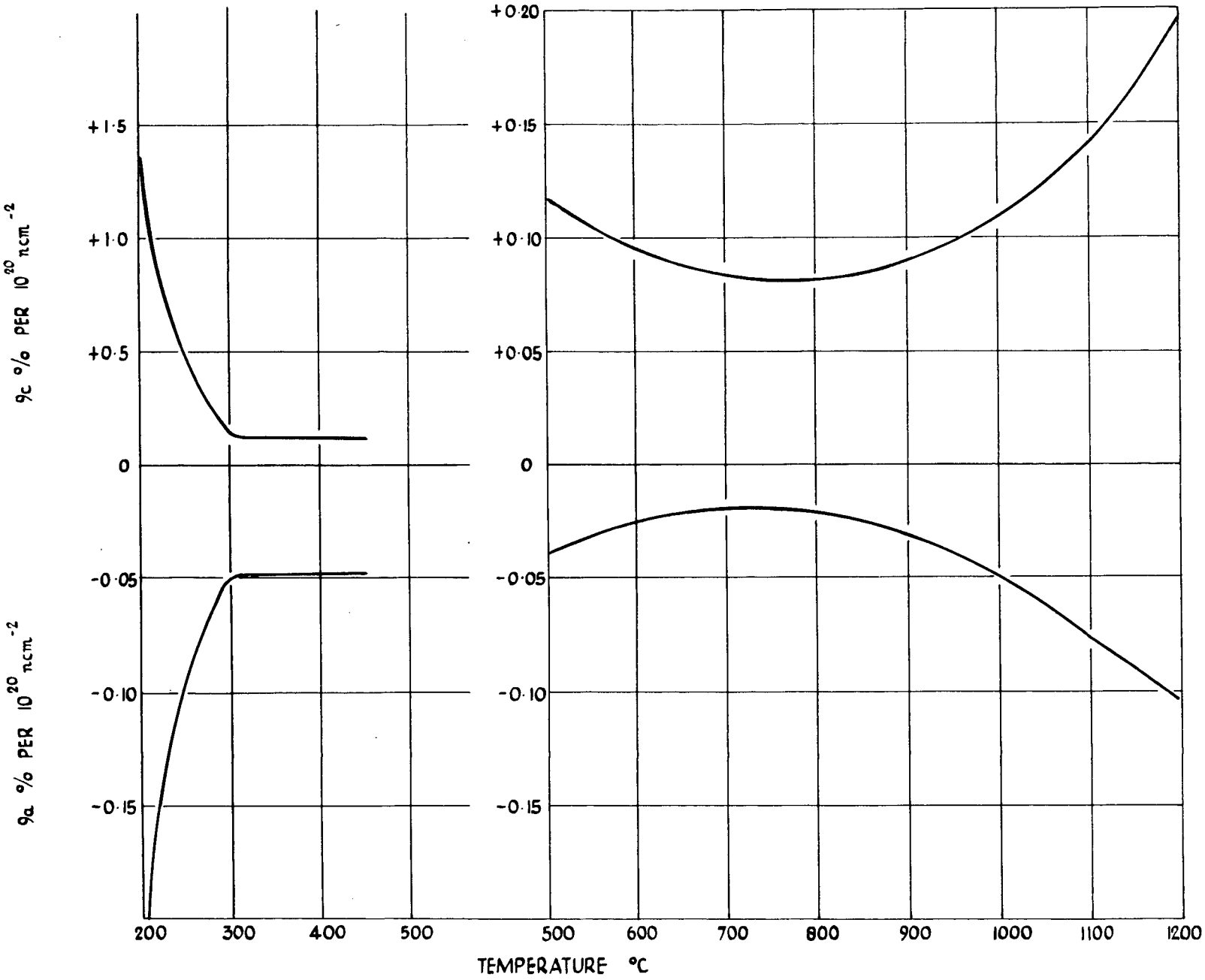

FIG. 1 CRYSTALLITE DIMENSIONAL CHANGES PRODUCED BY IRRADIATION IN A GRAPHITE WITH A WELL-DEVELOPED CRYSTAL STRUCTURE.

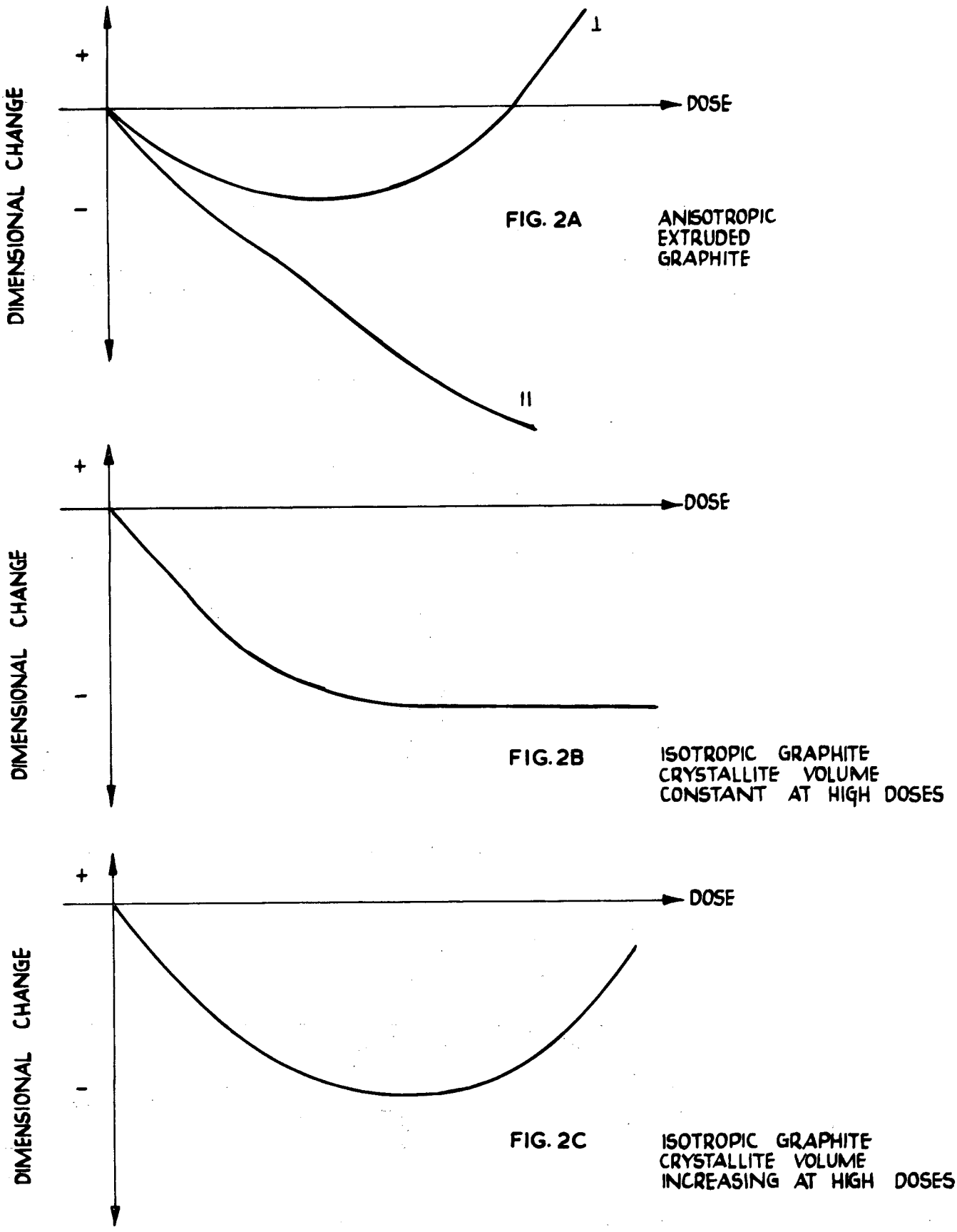

FIG. 2A ANISOTROPIC EXTRUDED GRAPHITE

FIG. 2B ISOTROPIC GRAPHITE CRYSTALLITE VOLUME CONSTANT AT HIGH DOSES

FIG. 2C ISOTROPIC GRAPHITE CRYSTALLITE VOLUME INCREASING AT HIGH DOSES

FIG. 2 SCHEMATIC REPRESENTATION OF TYPES OF DIMENSIONAL CHANGES PRODUCED BY IRRADIATION

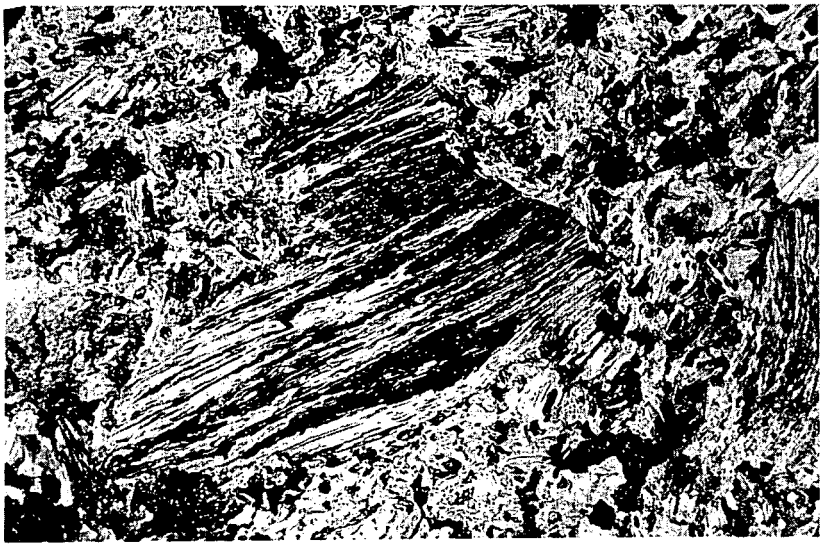

X75

Fig. 3(a) Coarse Grained Anisotropic

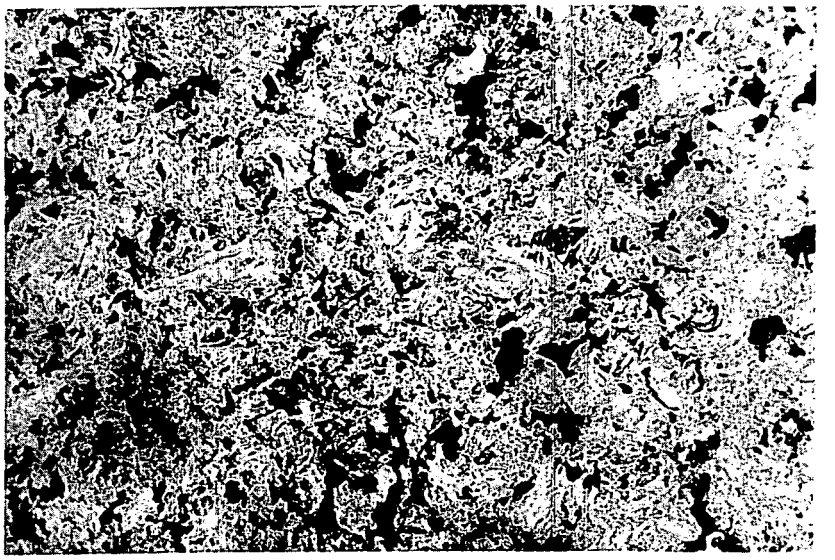

X75

Fig. 3(b) Fine Grained Anisotropic

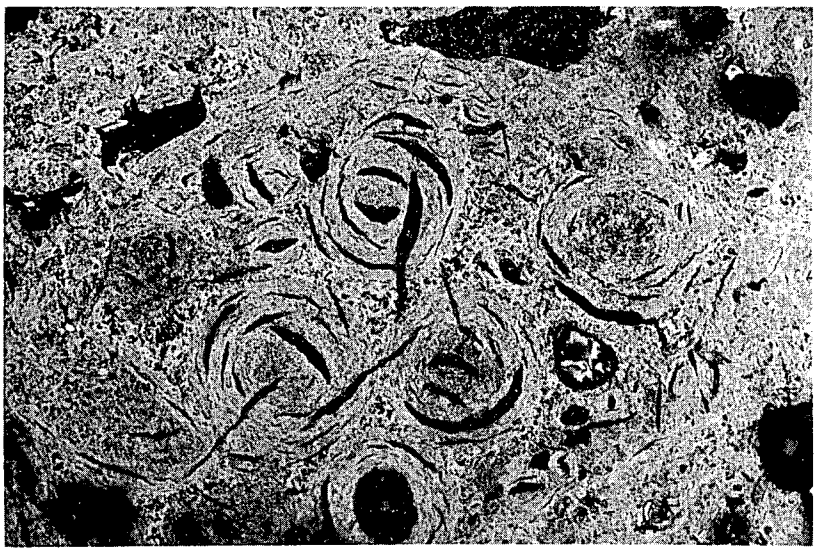

X75

Fig. 3(c) Spherical Grist Isotropic

X75

Fig. 3(d) Very Fine Grained Isotropic

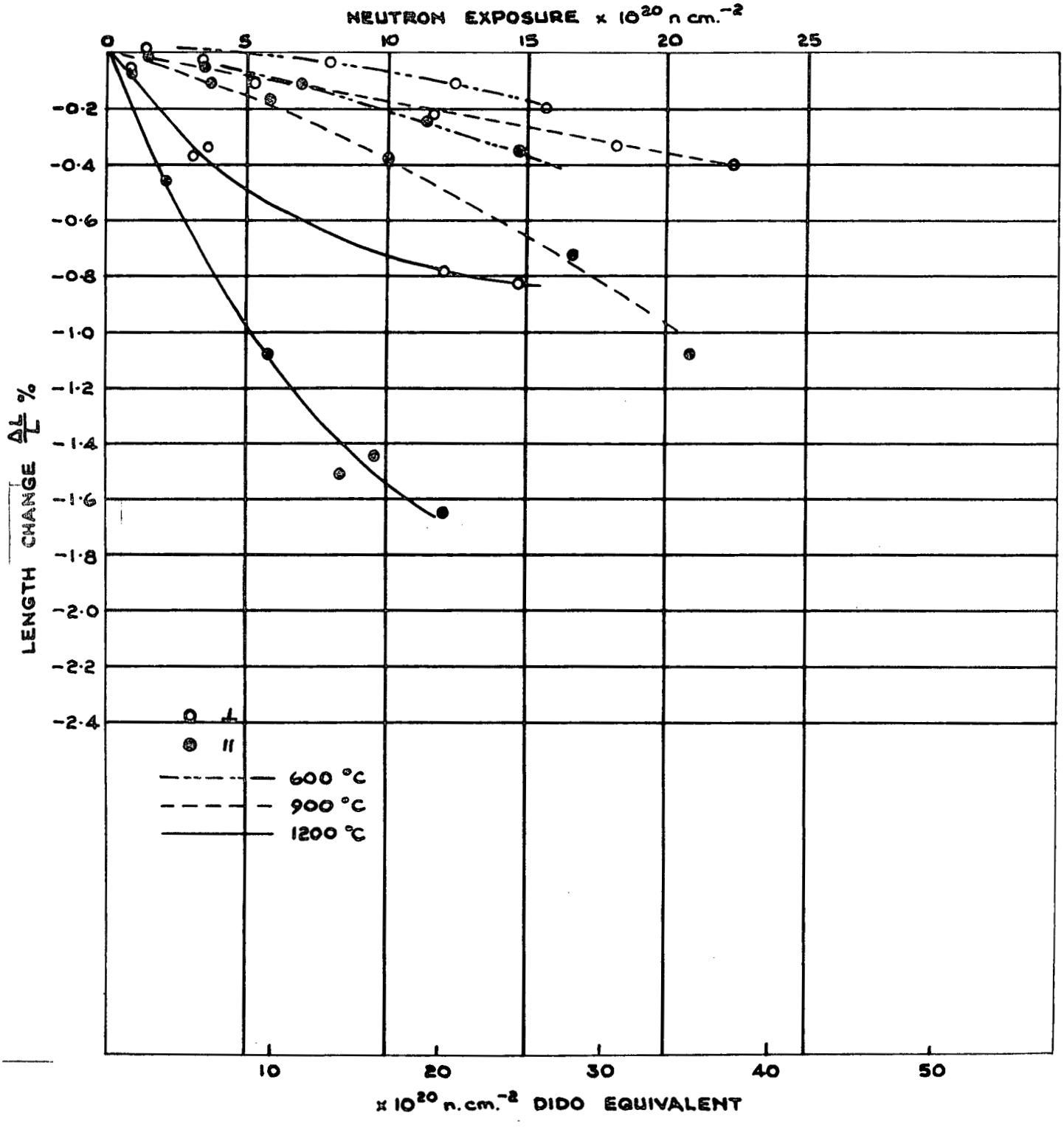

FIG. 4 DIMENSIONAL CHANGES OF GOO

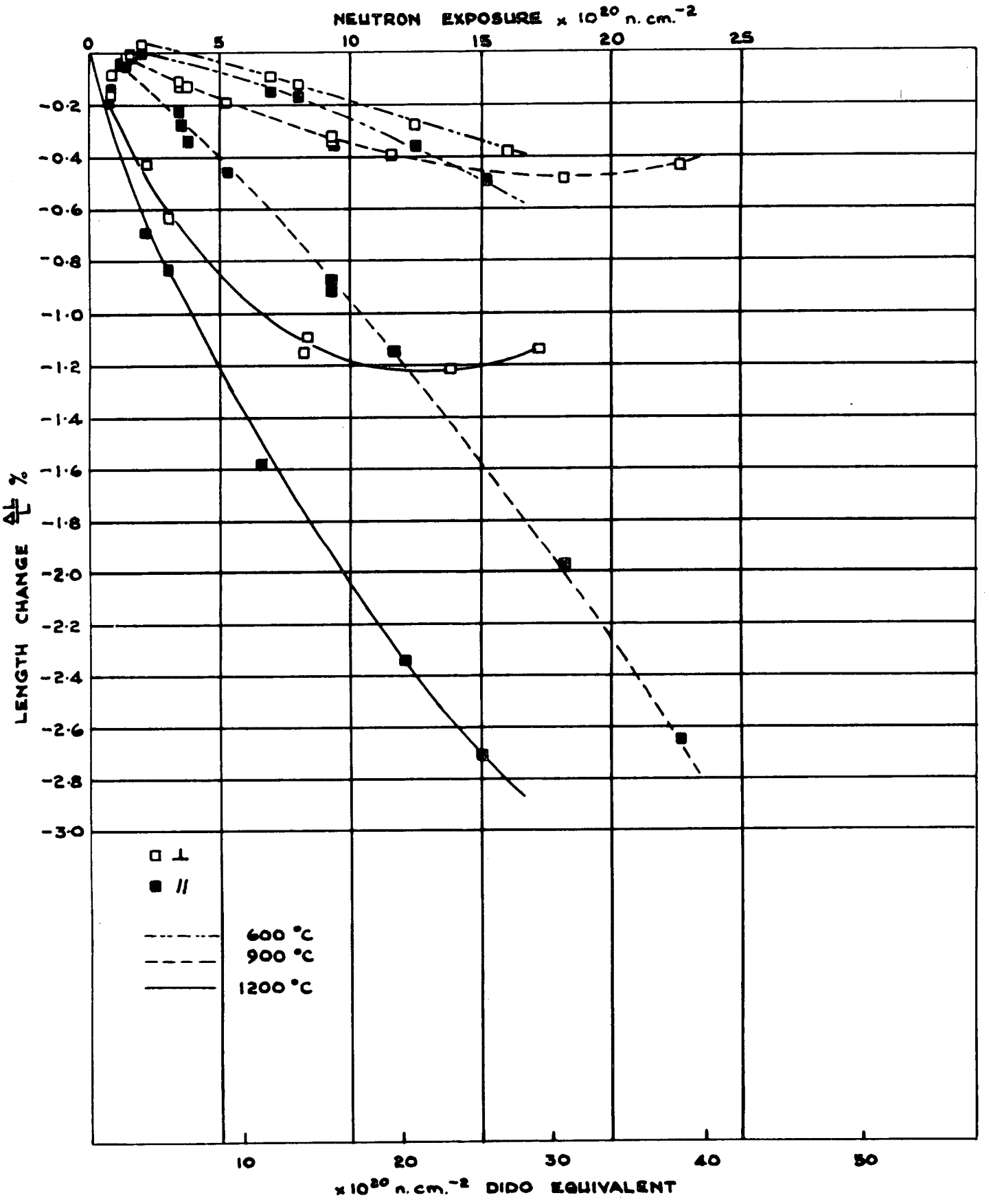

FIG. 5 DIMENSIONAL CHANGES OF G5

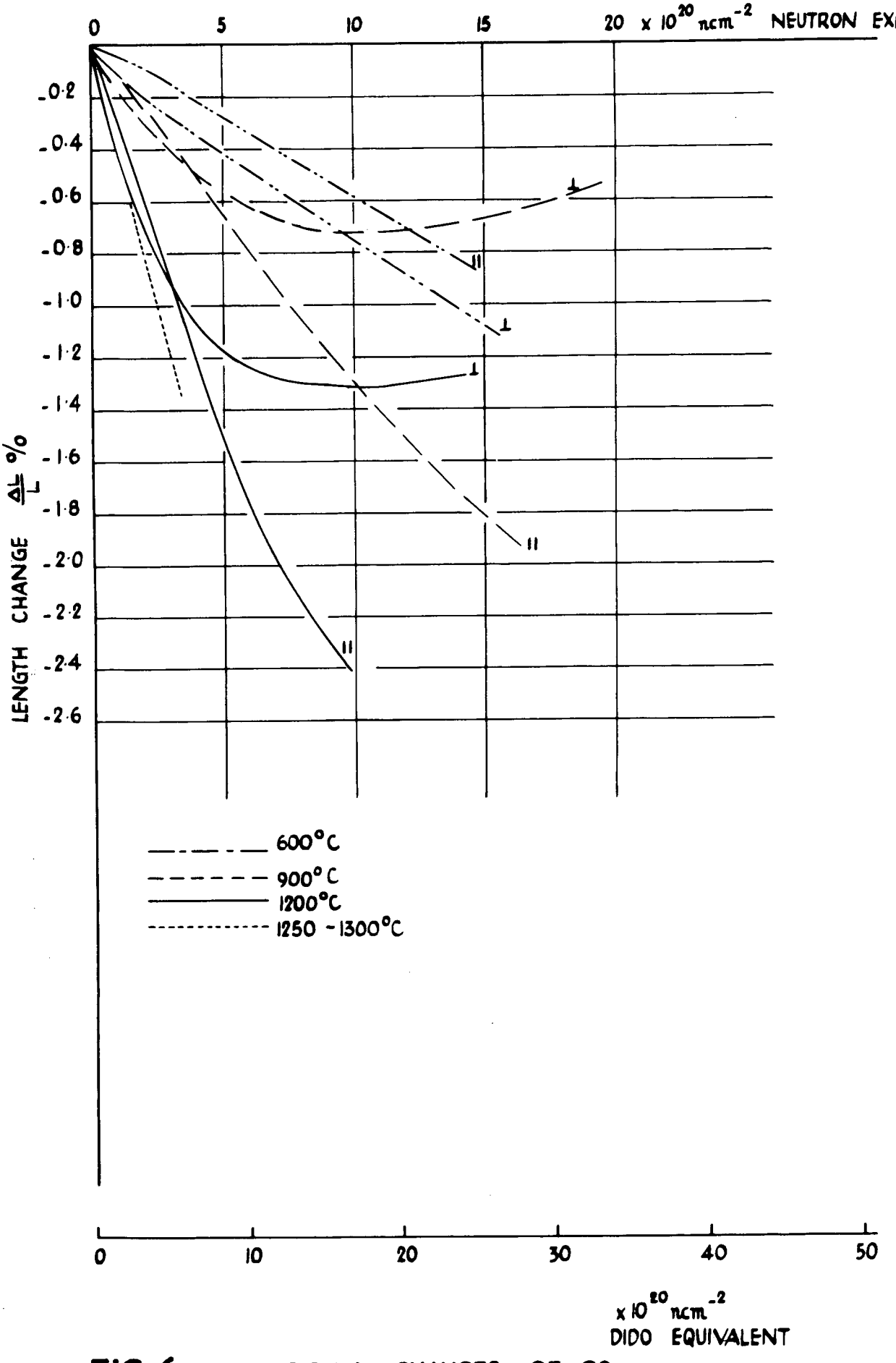

FIG. 6 DIMENSIONAL CHANGES OF G9

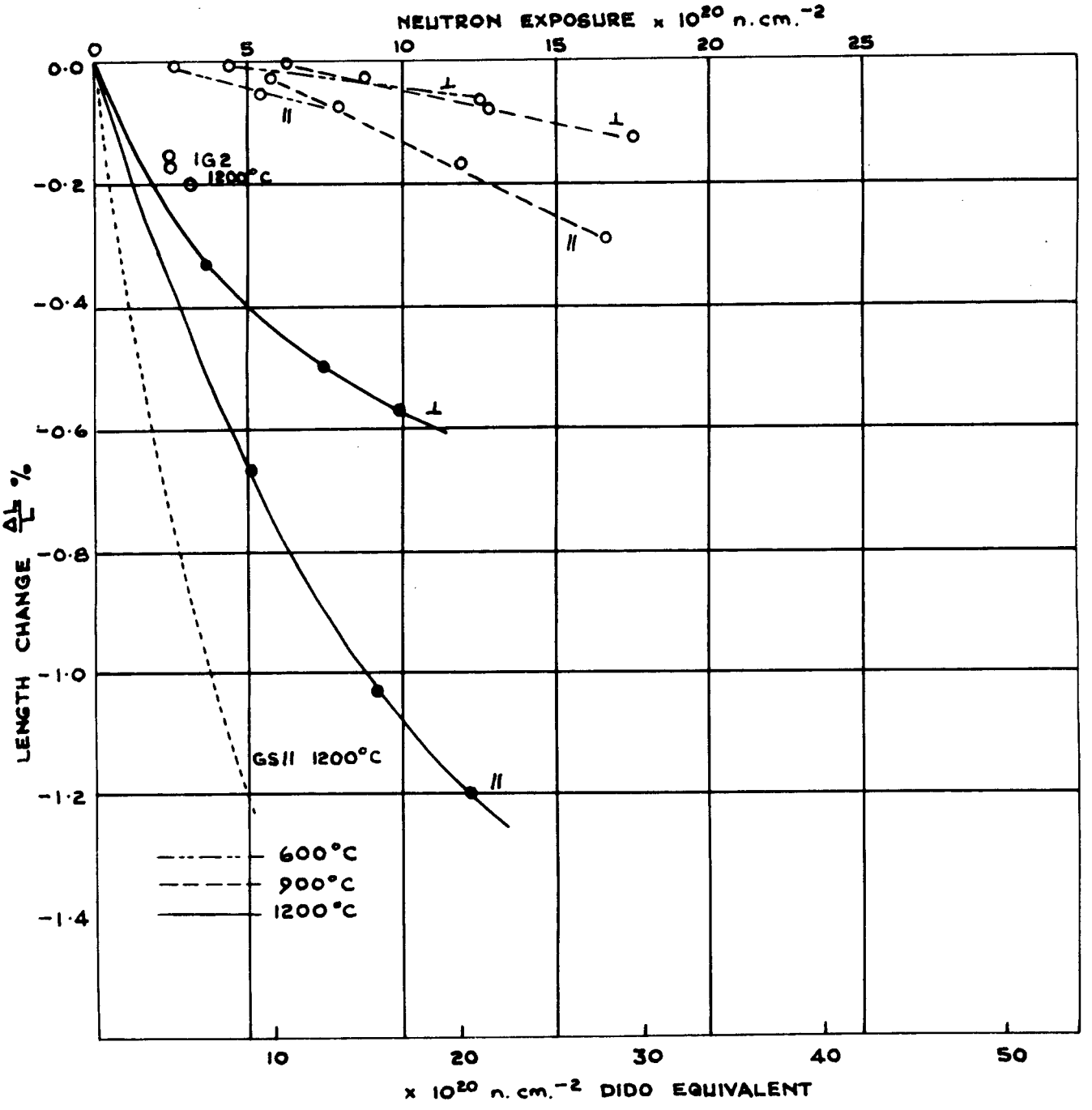

FIG.7 DIMENSIONAL CHANGES IG

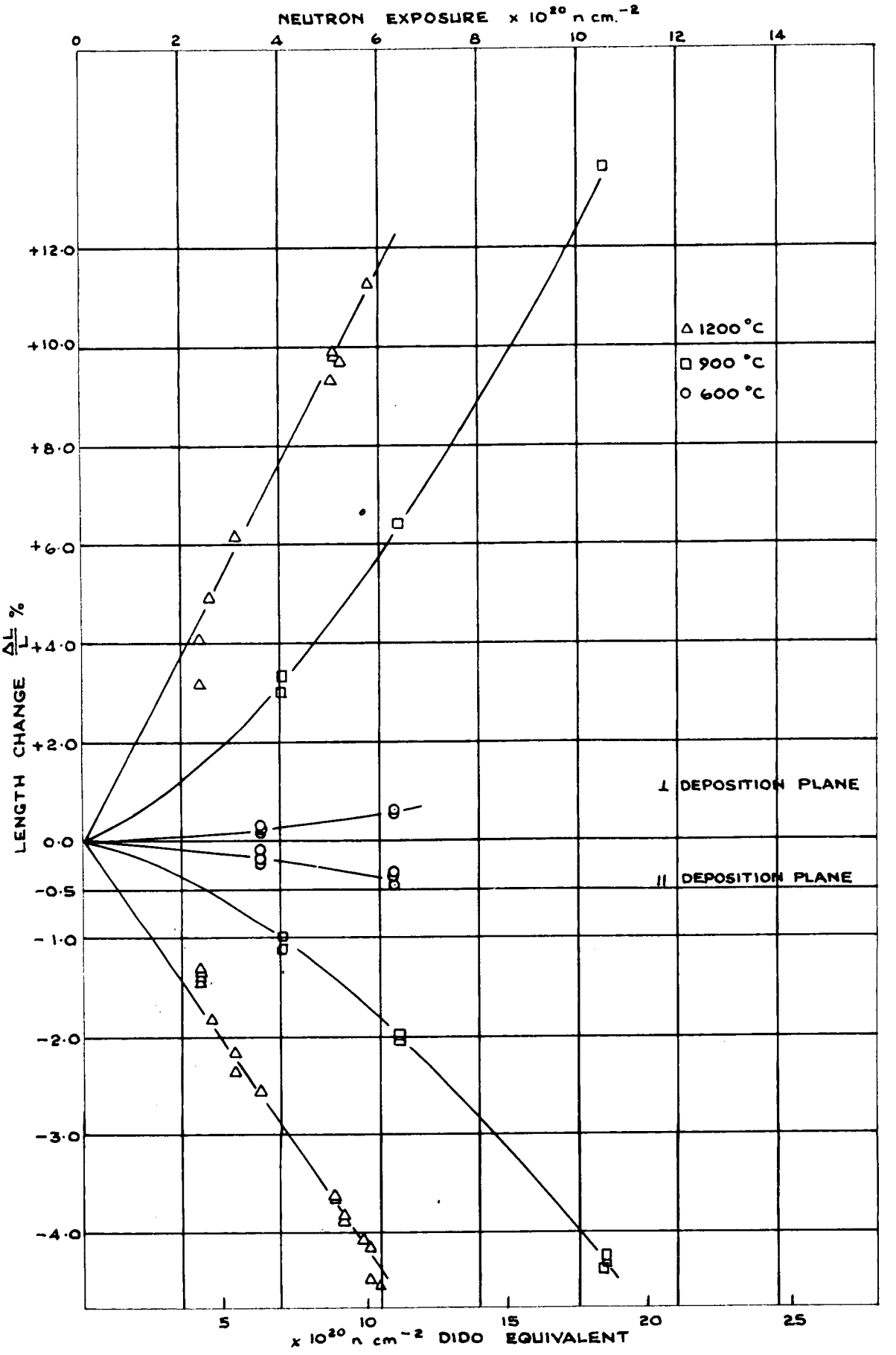

FIG. 8 DIMENSIONAL CHANGES OF PYROLYTIC GRAPHITE (58)

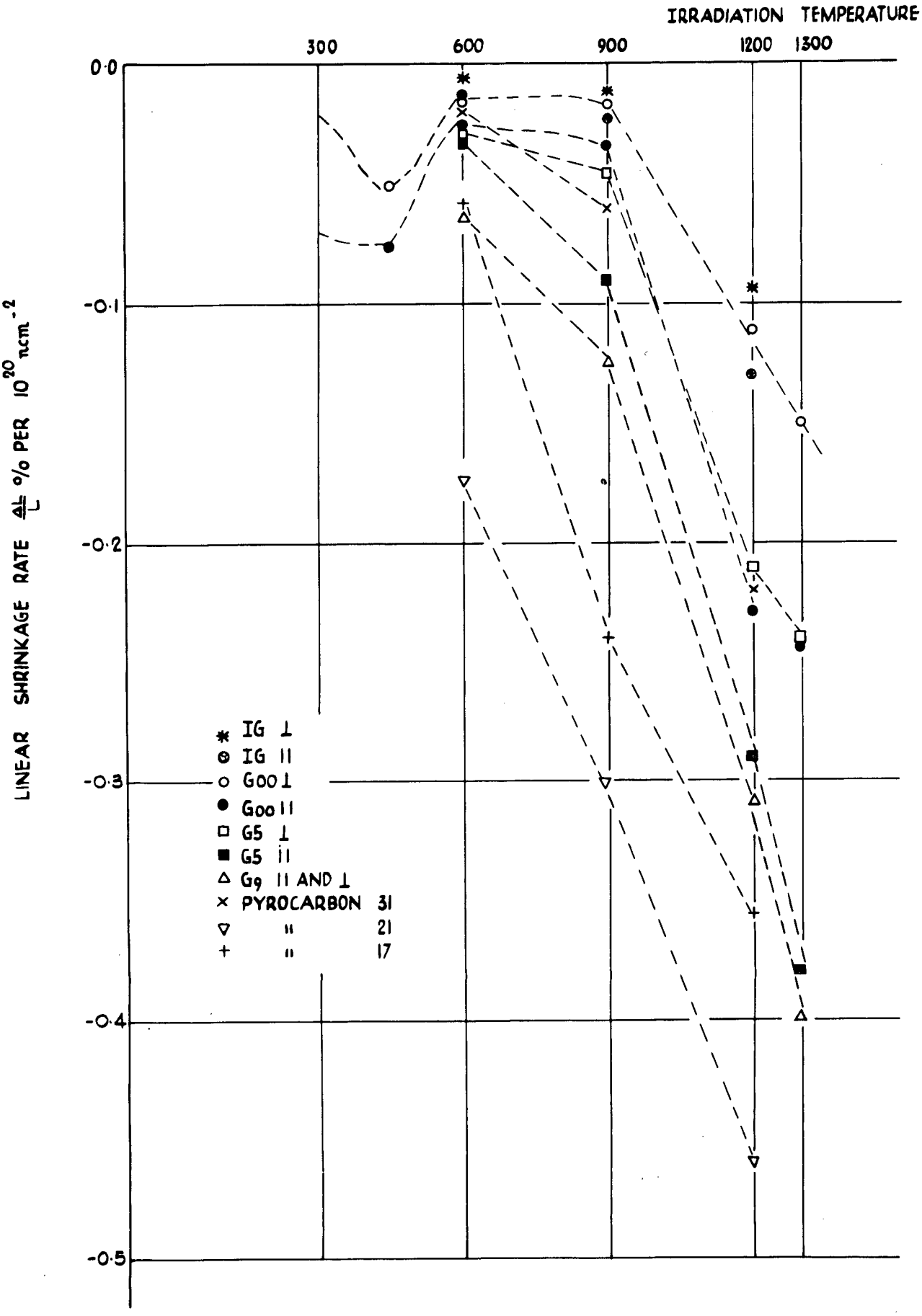

FIG. 9 INITIAL CONTRACTION RATES AS A FUNCTION OF TEMPERATURE

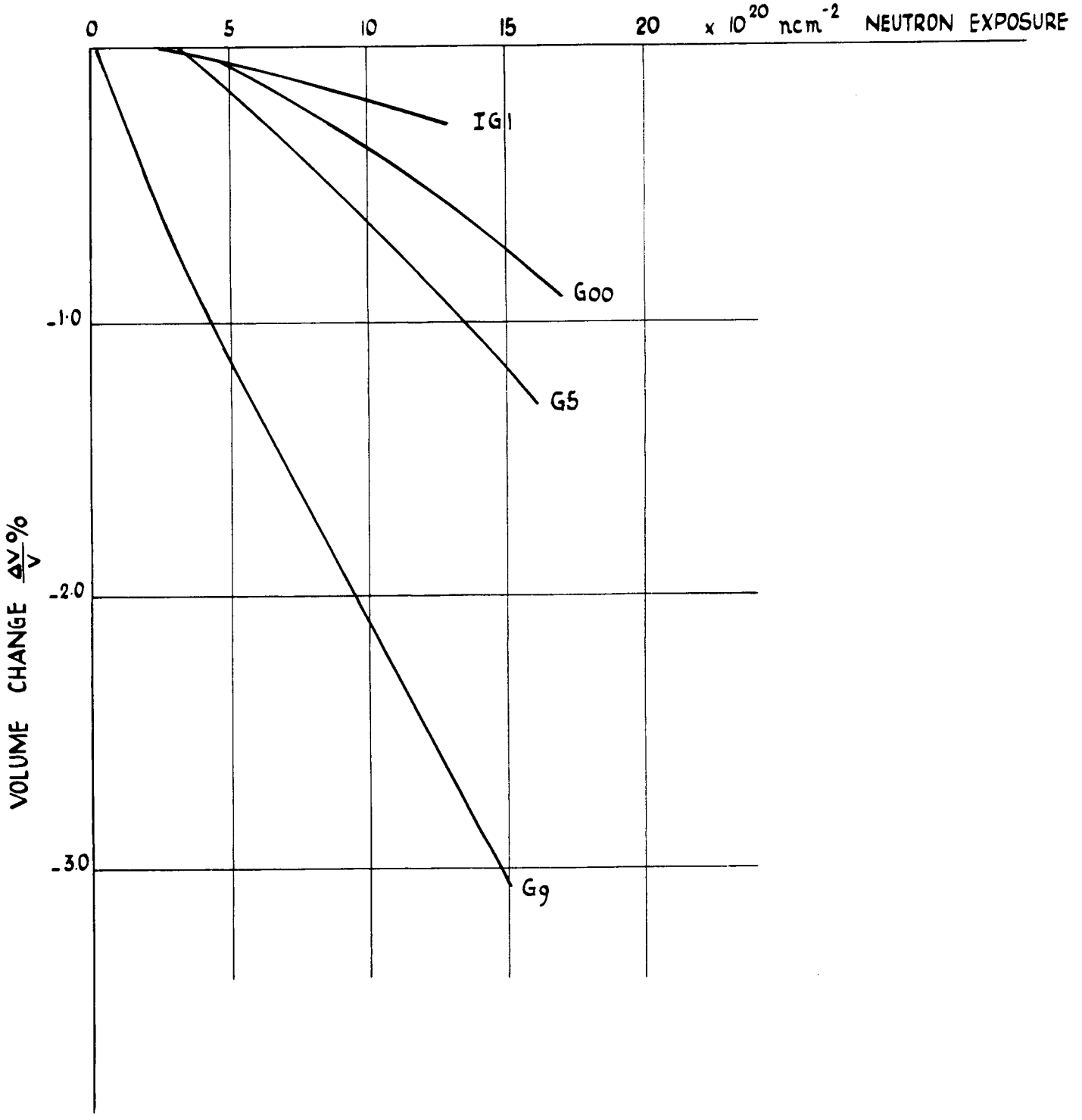

FIG. 10 BULK VOLUME CHANGES 600°C

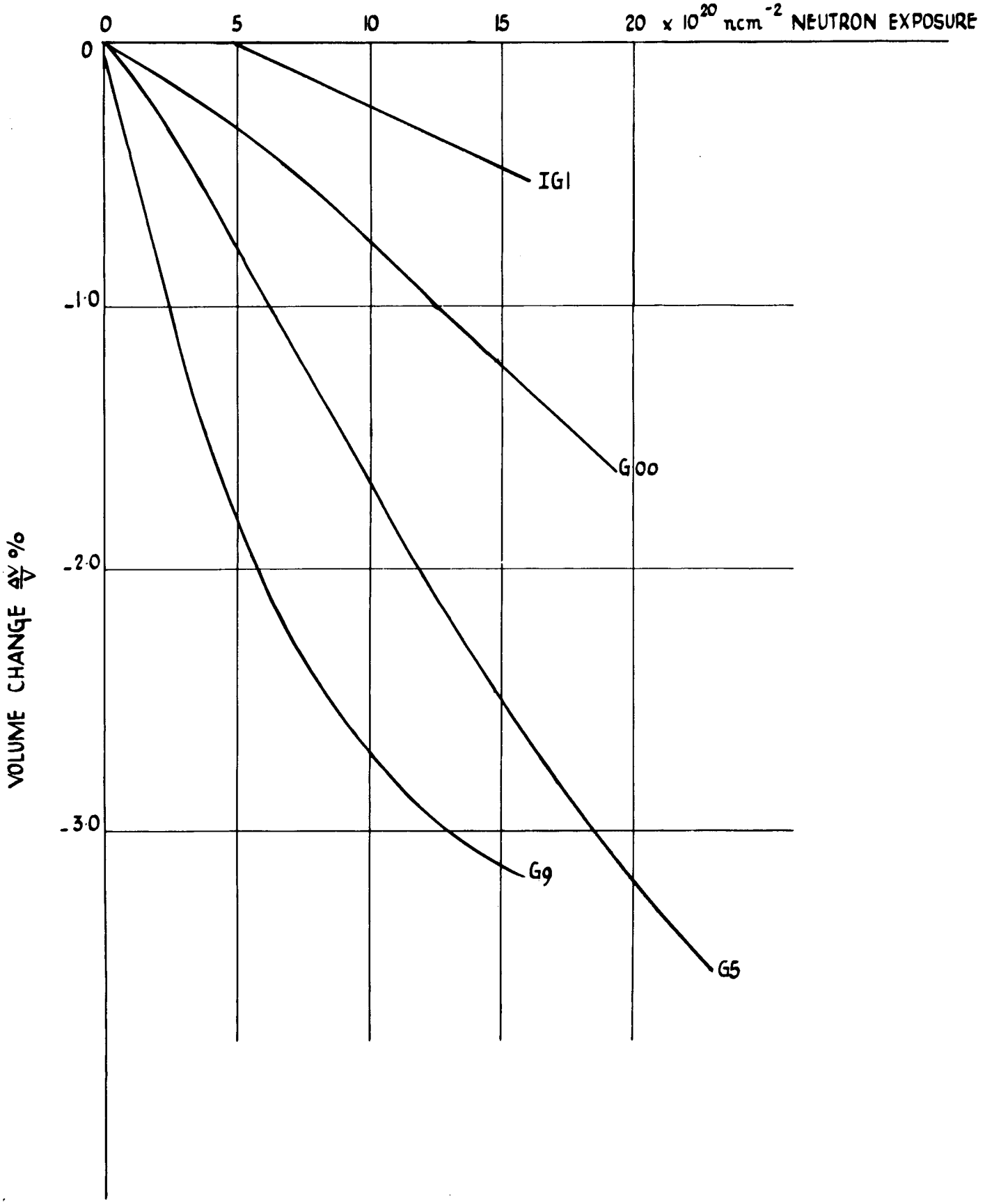

FIG. 11 BULK VOLUME CHANGES 900°C

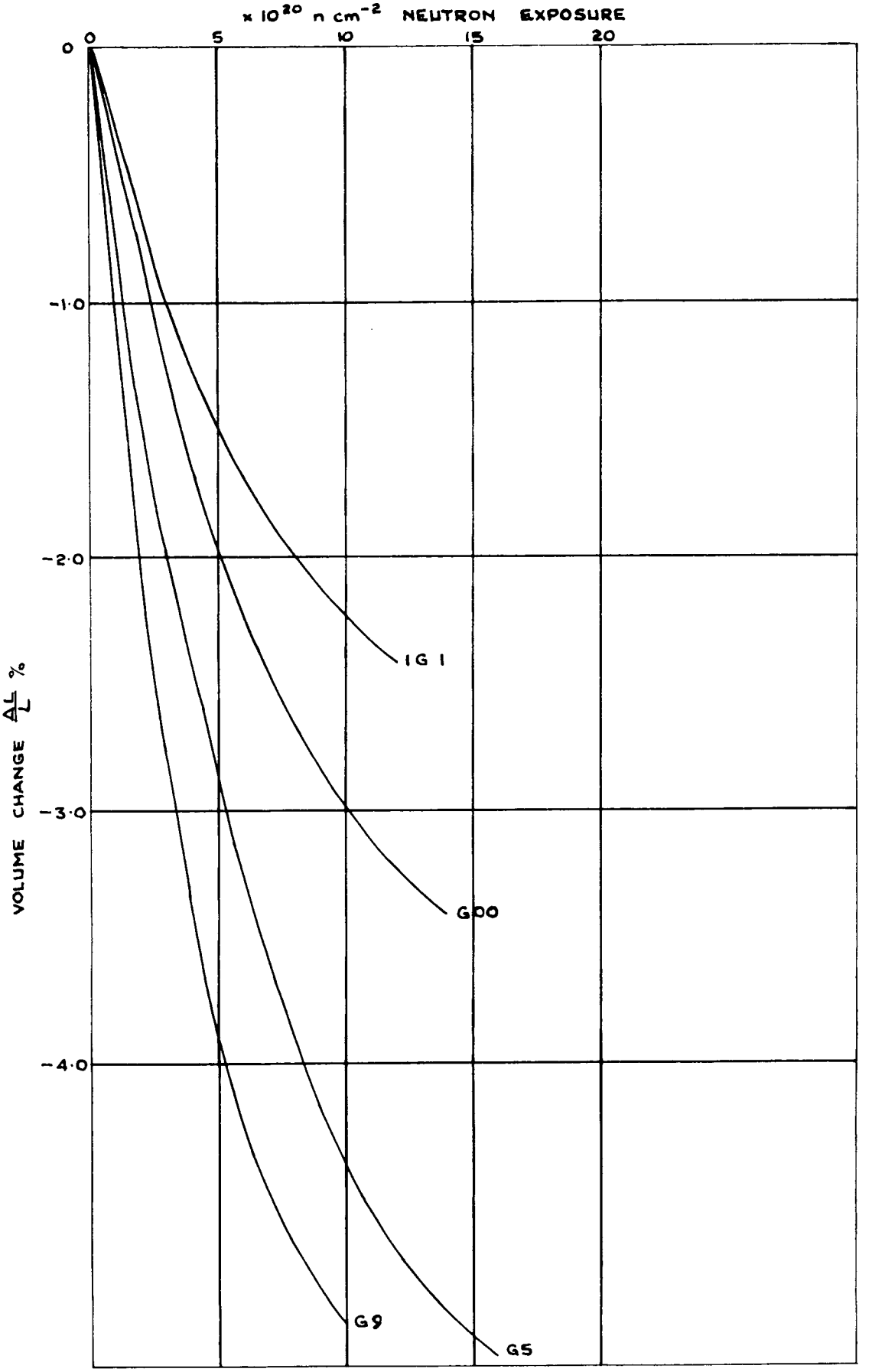

FIG. 12 BULK VOLUME CHANGES 1200 °C

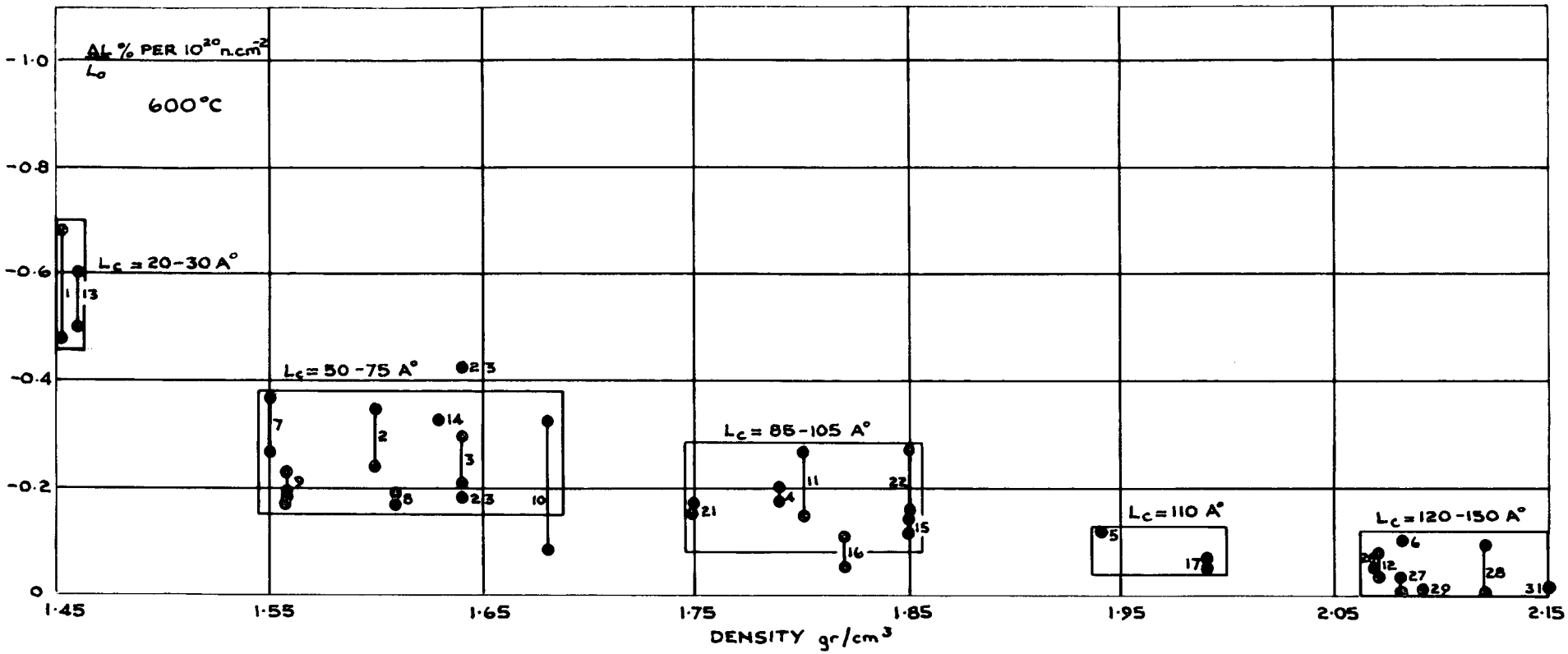

FIG 13A DRAGON PYROCARBON DISCS 600 °C
CONTRACTION RATE VERSUS DENSITY

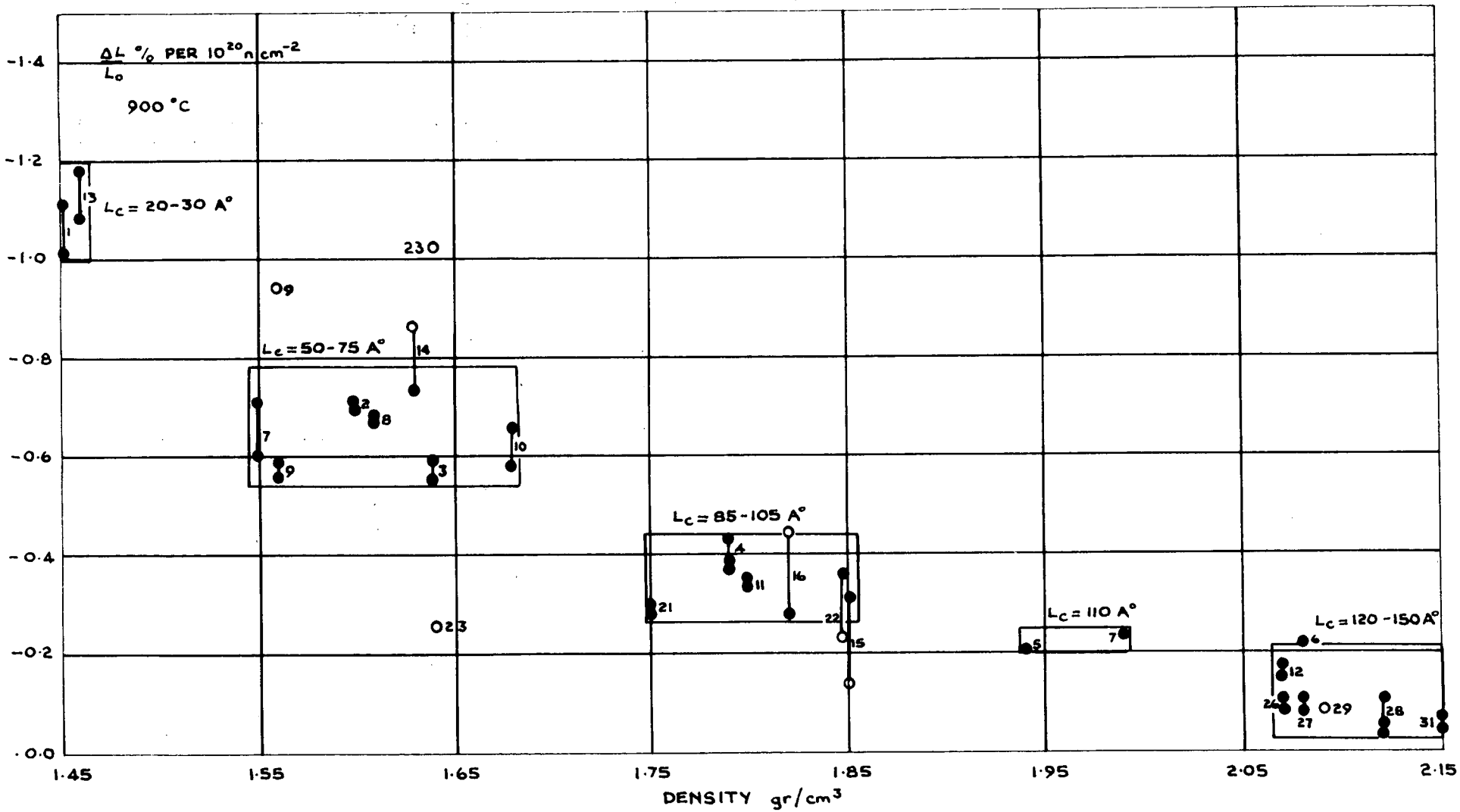

FIG 13B DRAGON PYROCARBON DISCS 900 °C
CONTRACTION RATE VERSUS DENSITY

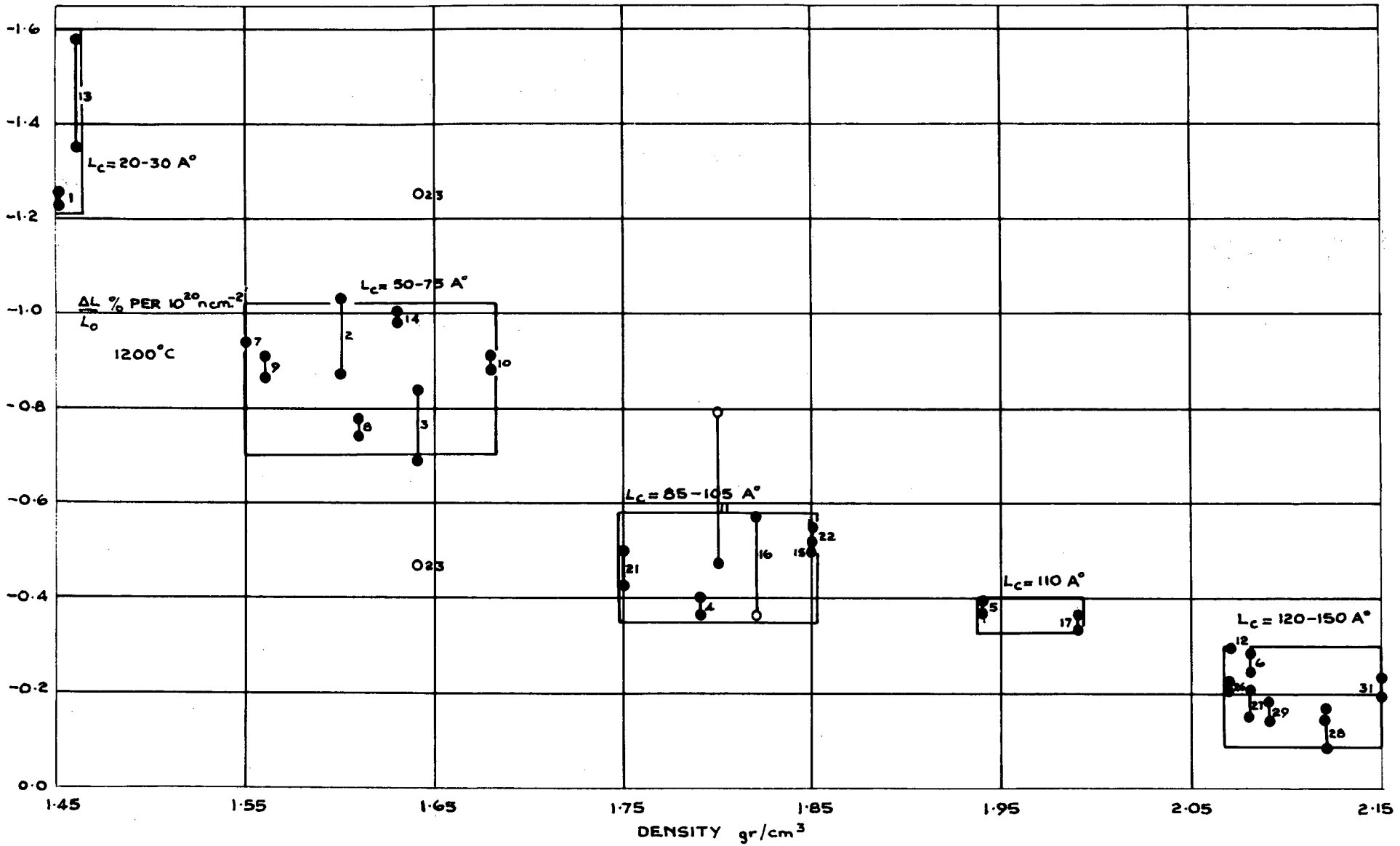

FIG 13C DRAGON PYROCARBON DISCS 1200 °C
CONTRACTION RATE VERSUS DENSITY

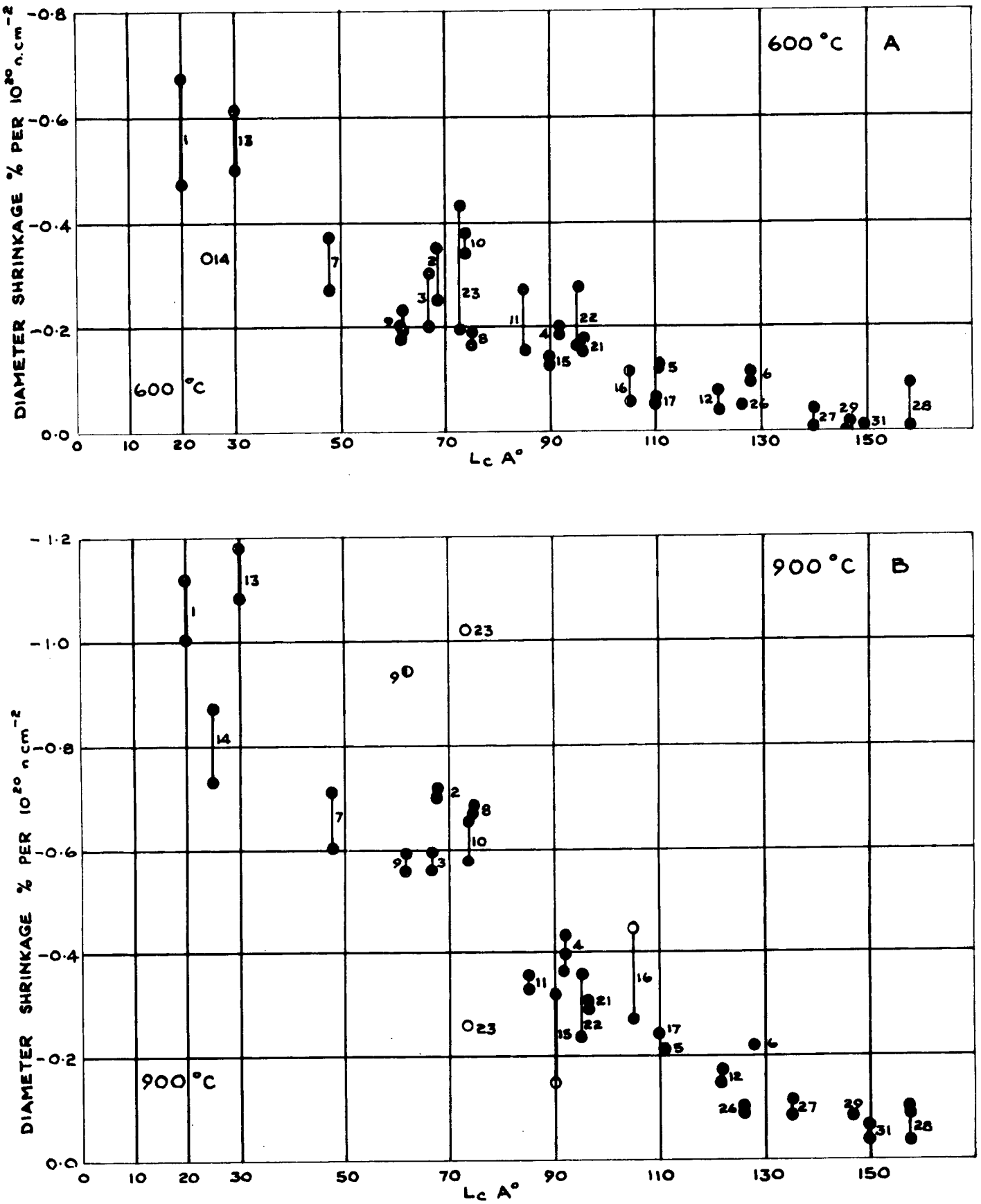

FIG. 14 A & 14 B DRAGON PYROCARBON DISCS 900°C & 600°C

CONTRACTION RATES VERSUS CRYSTALLITE HEIGHT

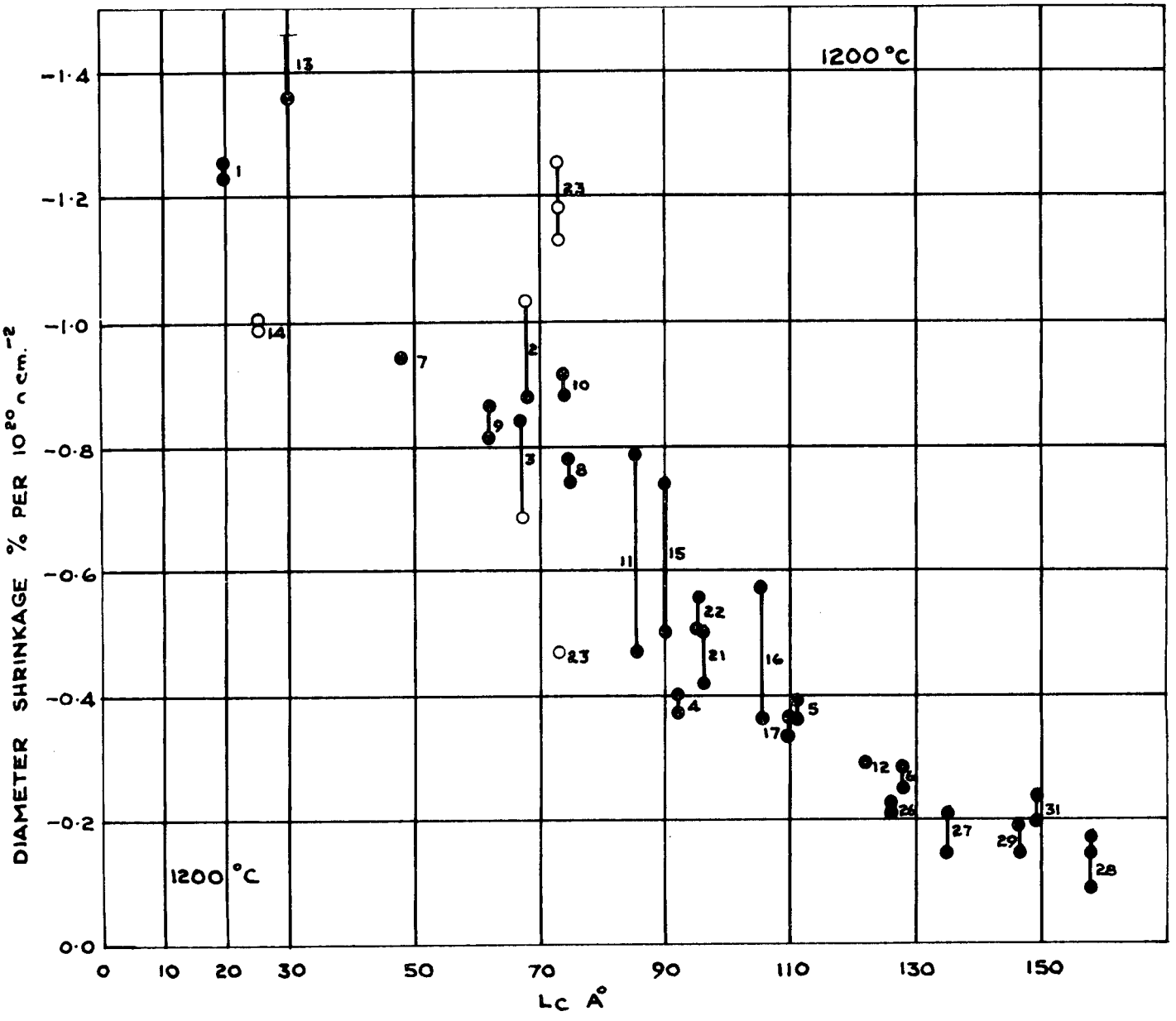

FIG. 14 C CONTRACTION RATE VERSUS CRYSTALLITE HEIGHT

DRAGON PYROCARBON DISCS 1200 °C

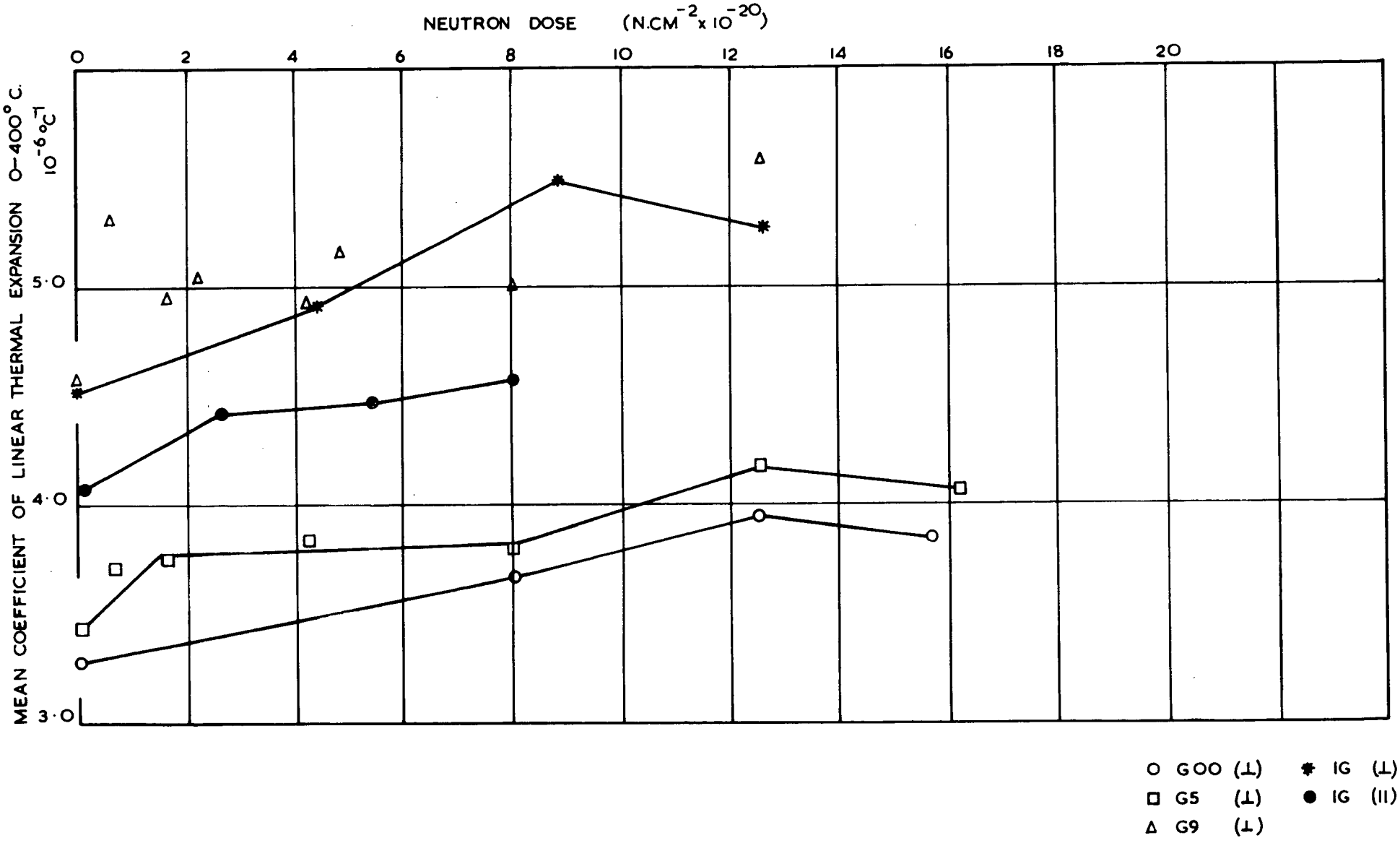

FIGURE 15A.
COEFFICIENT OF THERMAL EXPANSION AFTER IRRADIATION AT 600° C.

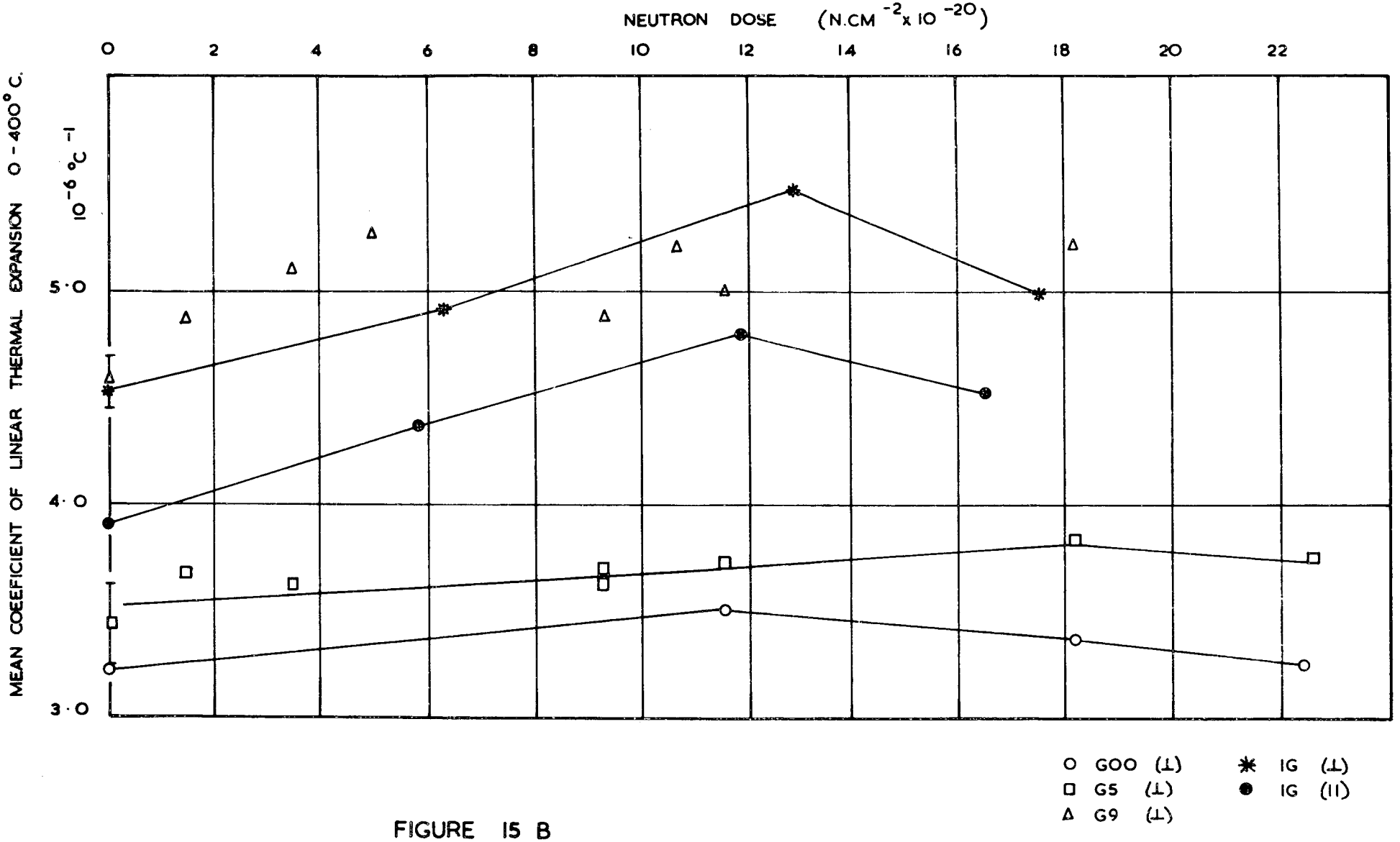

FIGURE 15 B

COEFFICIENT OF THERMAL EXPANSION AFTER IRRADIATION AT 900° C.

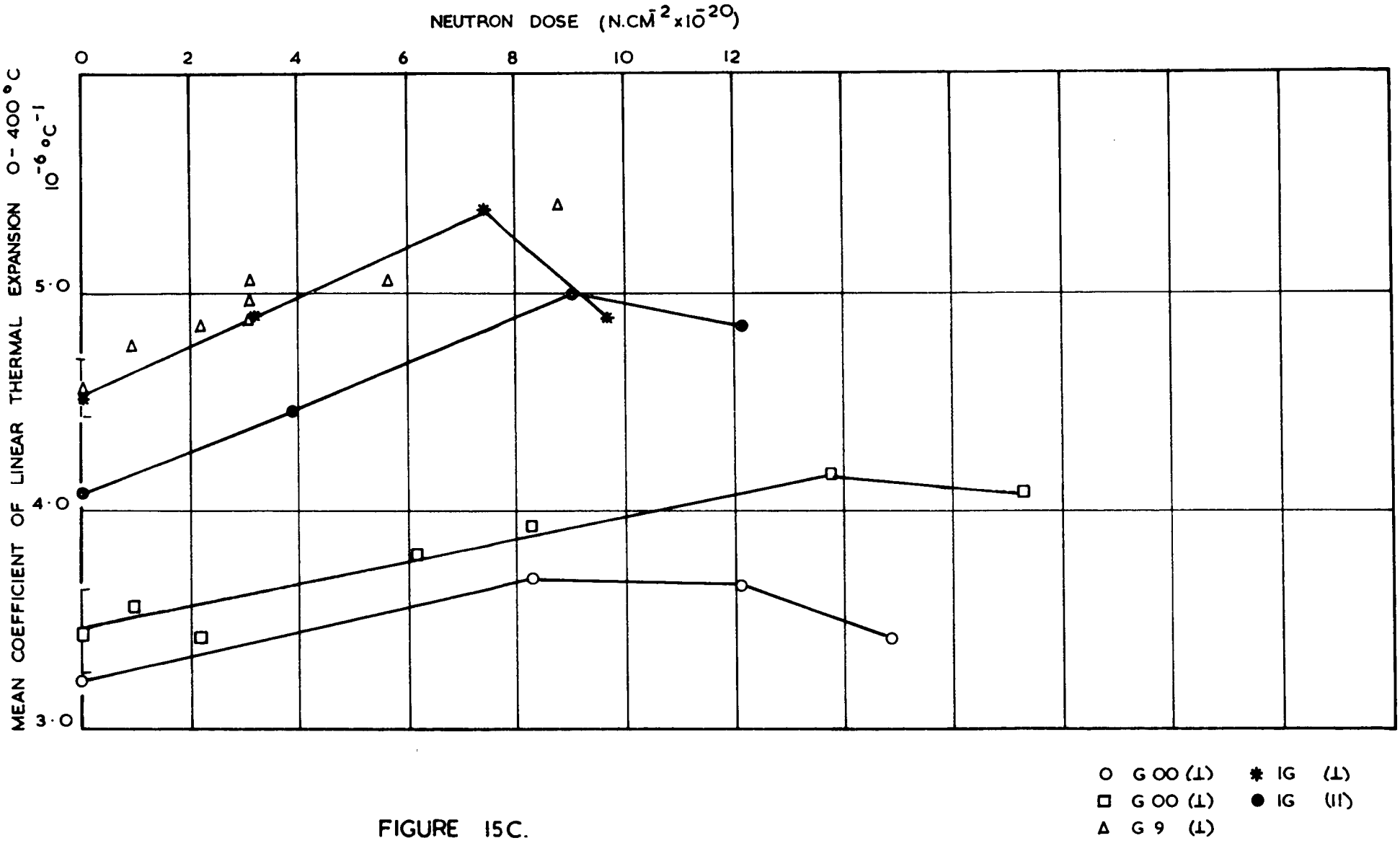

FIGURE 15C.
COEFFICIENT OF THERMAL EXPANSION AFTER IRRADIATION AT 1200° C.

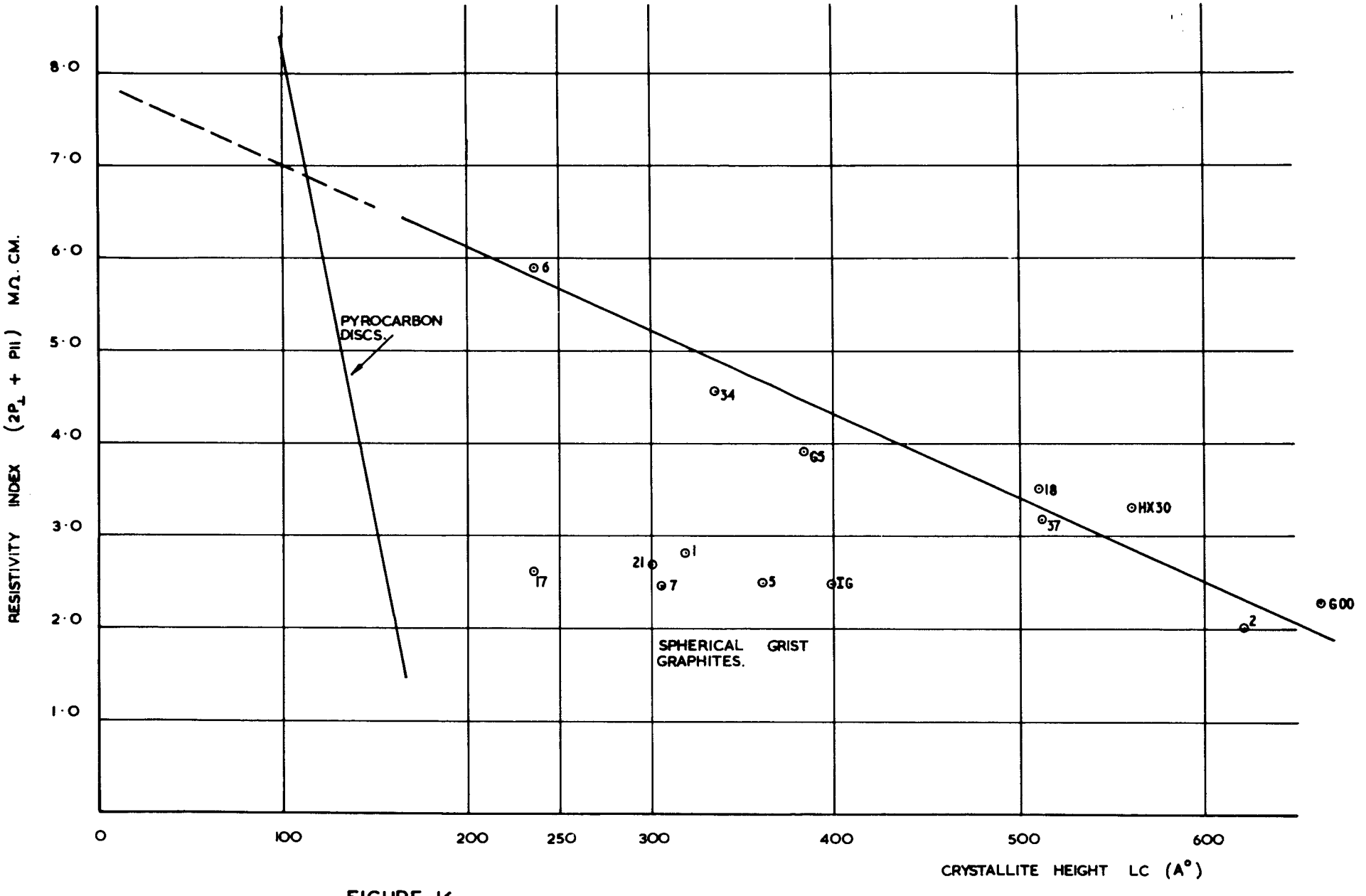

FIGURE 16.

ELECTRICAL RESISTIVITY INDEX VERSUS CRYSTALLITE HEIGHT FOR VARIOUS GRAPHITES.

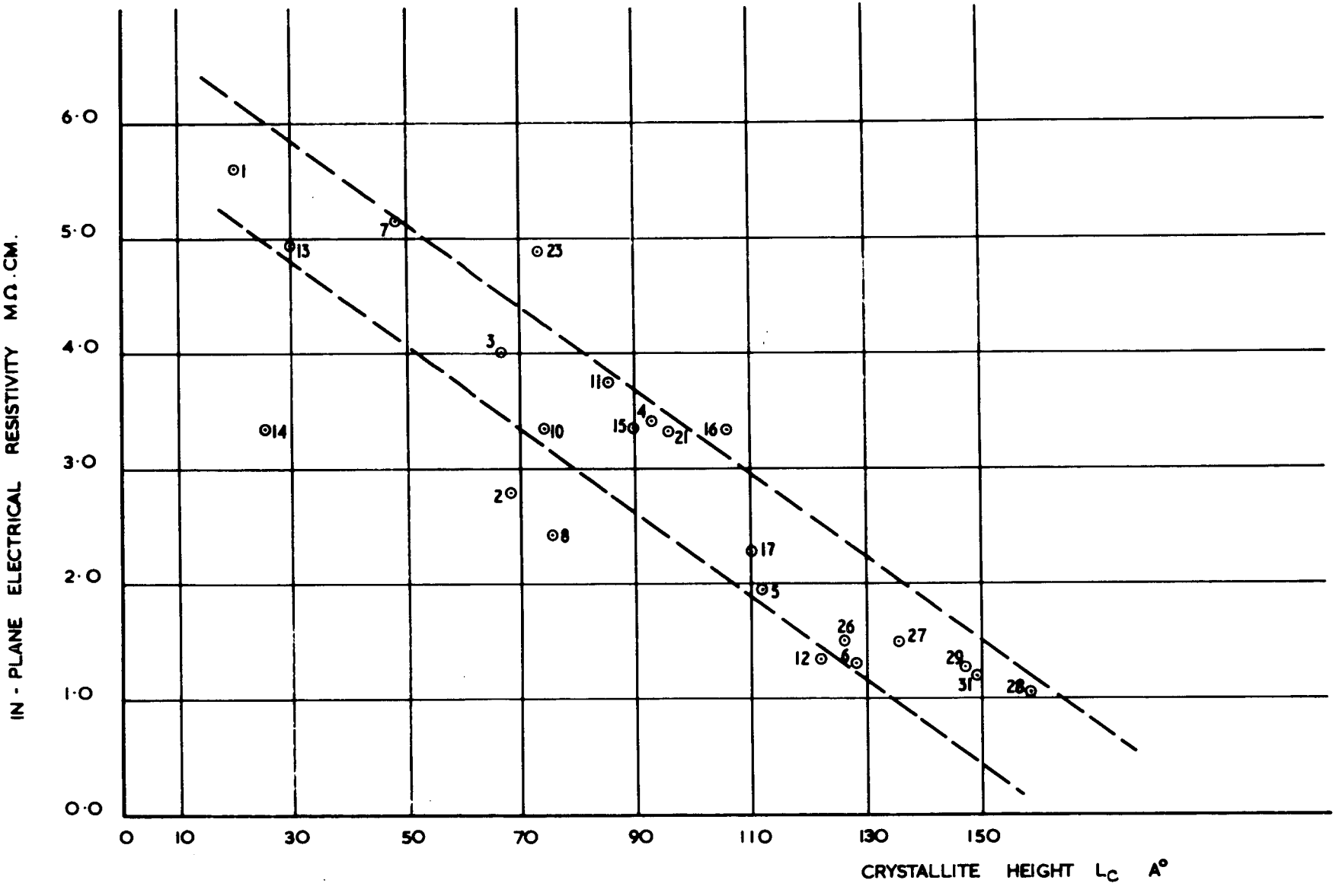

FIGURE 17.
DRAGON PYROCARBON DISCS.
ELECTRICAL RESISTIVITY VS CRYSTALLITE HEIGHT L_C

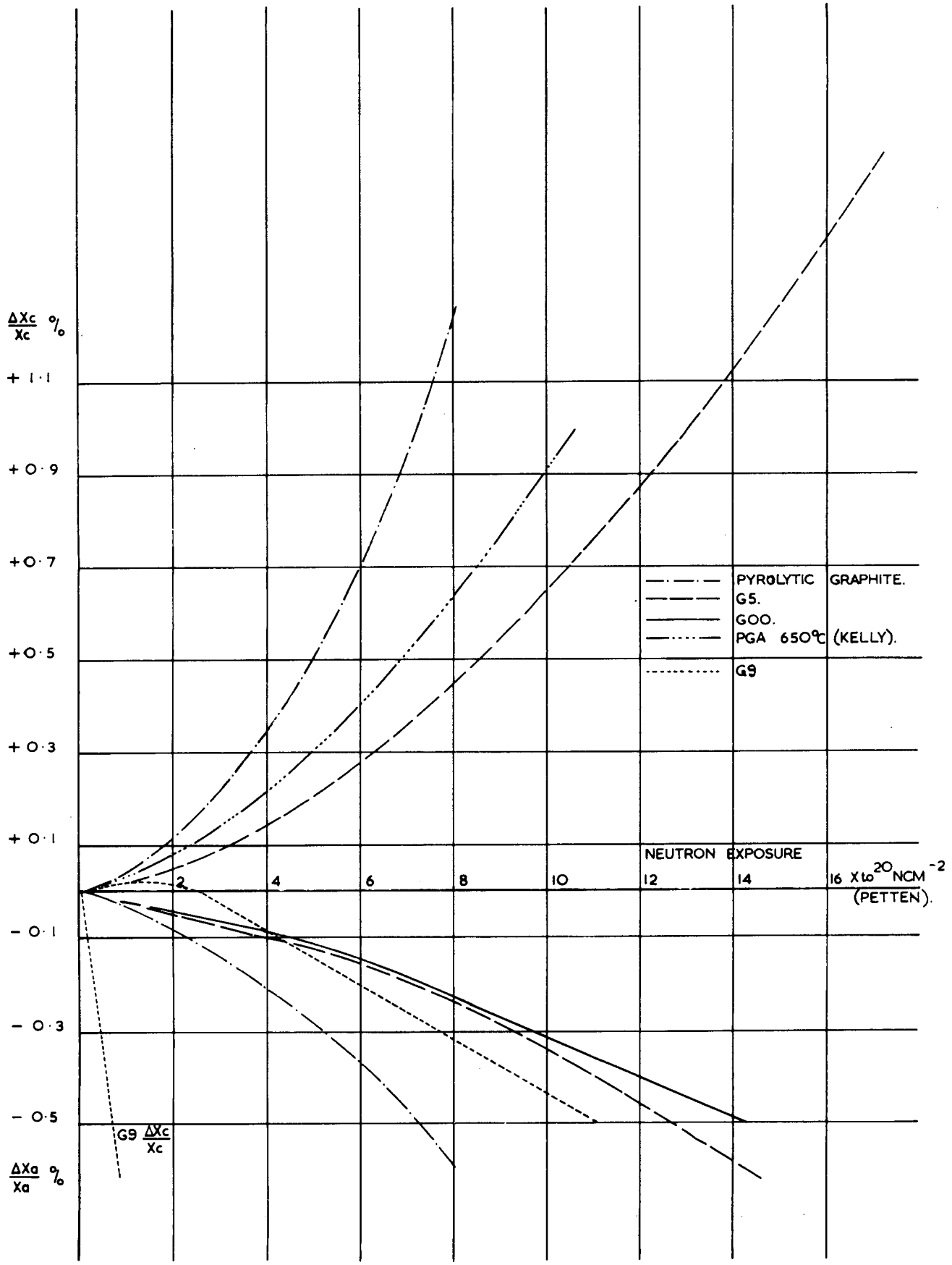

FIGURE 18.
APPARENT CRYSTALLITE DIMENSIONAL CHANGES 600° C.
CALCULATED FROM BULK DIMENSIONAL CHANGES.

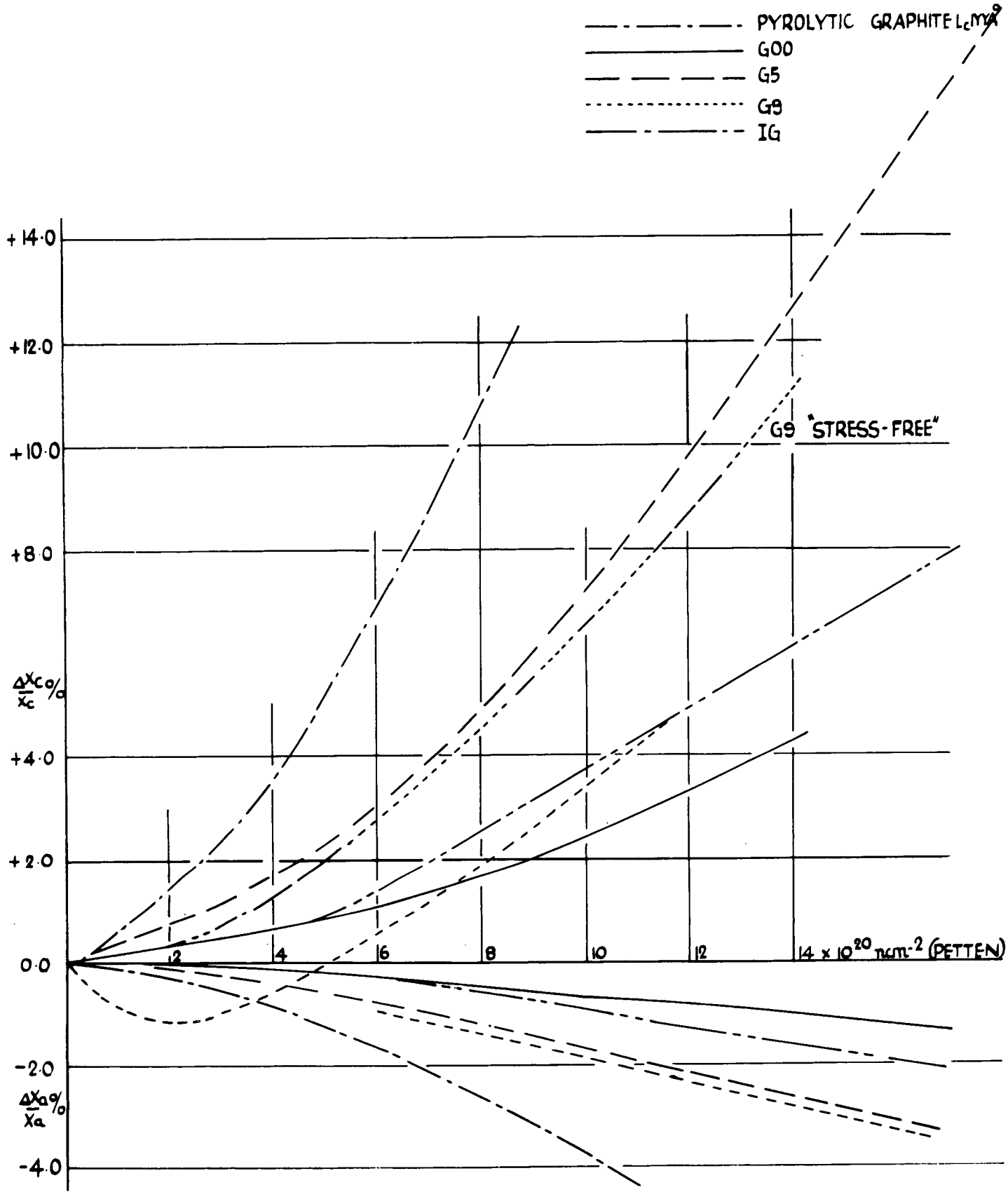

FIG. 19 APPARENT CRYSTALLITE DIMENSIONAL CHANGES 900°C CALCULATED FROM BULK DIMENSIONAL CHANGES

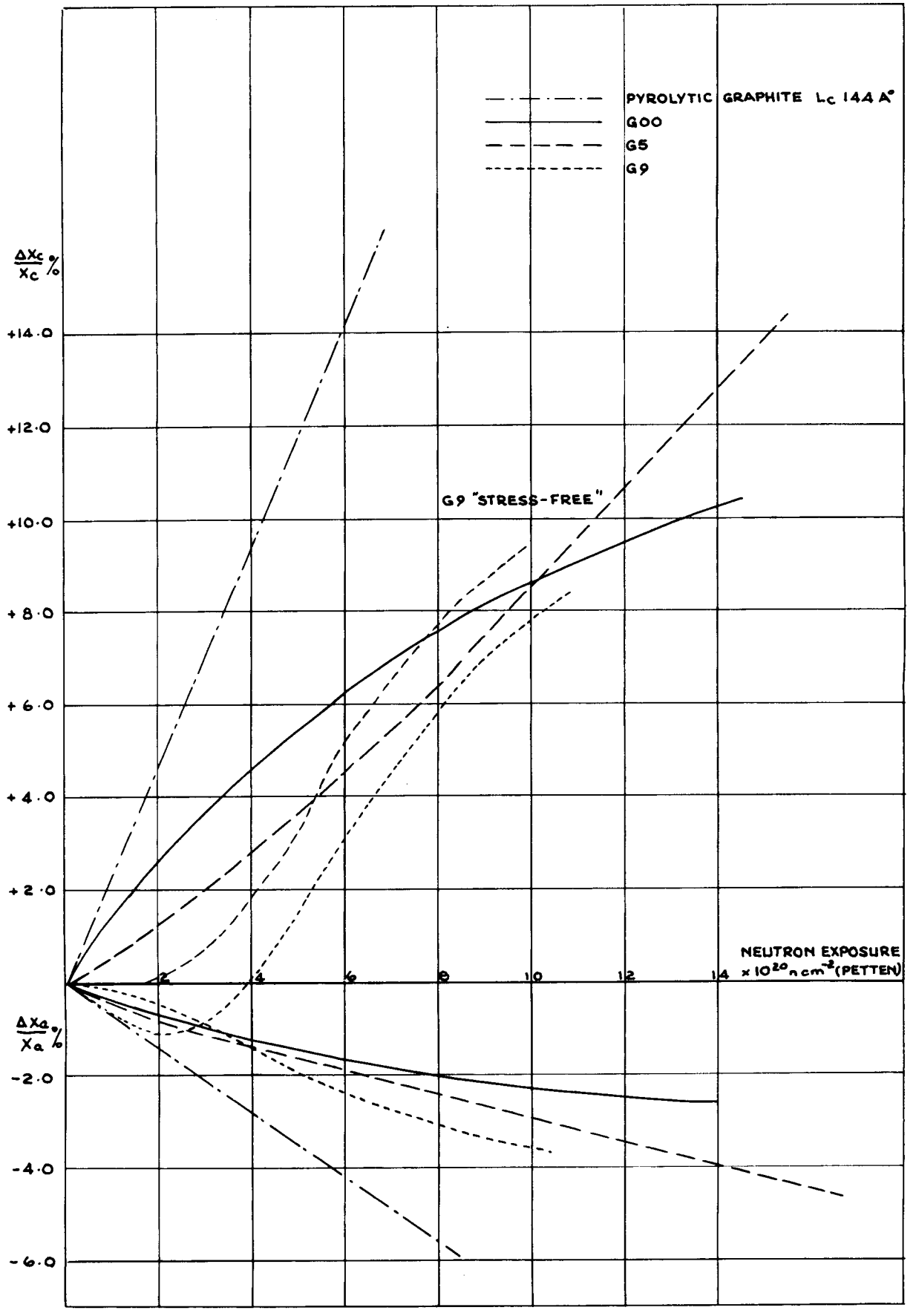

FIG. 20 APPARENT CRYSTALLITE DIMENSIONAL CHANGES 1200 °C CALCULATED FROM BULK DIMENSIONAL CHANGES

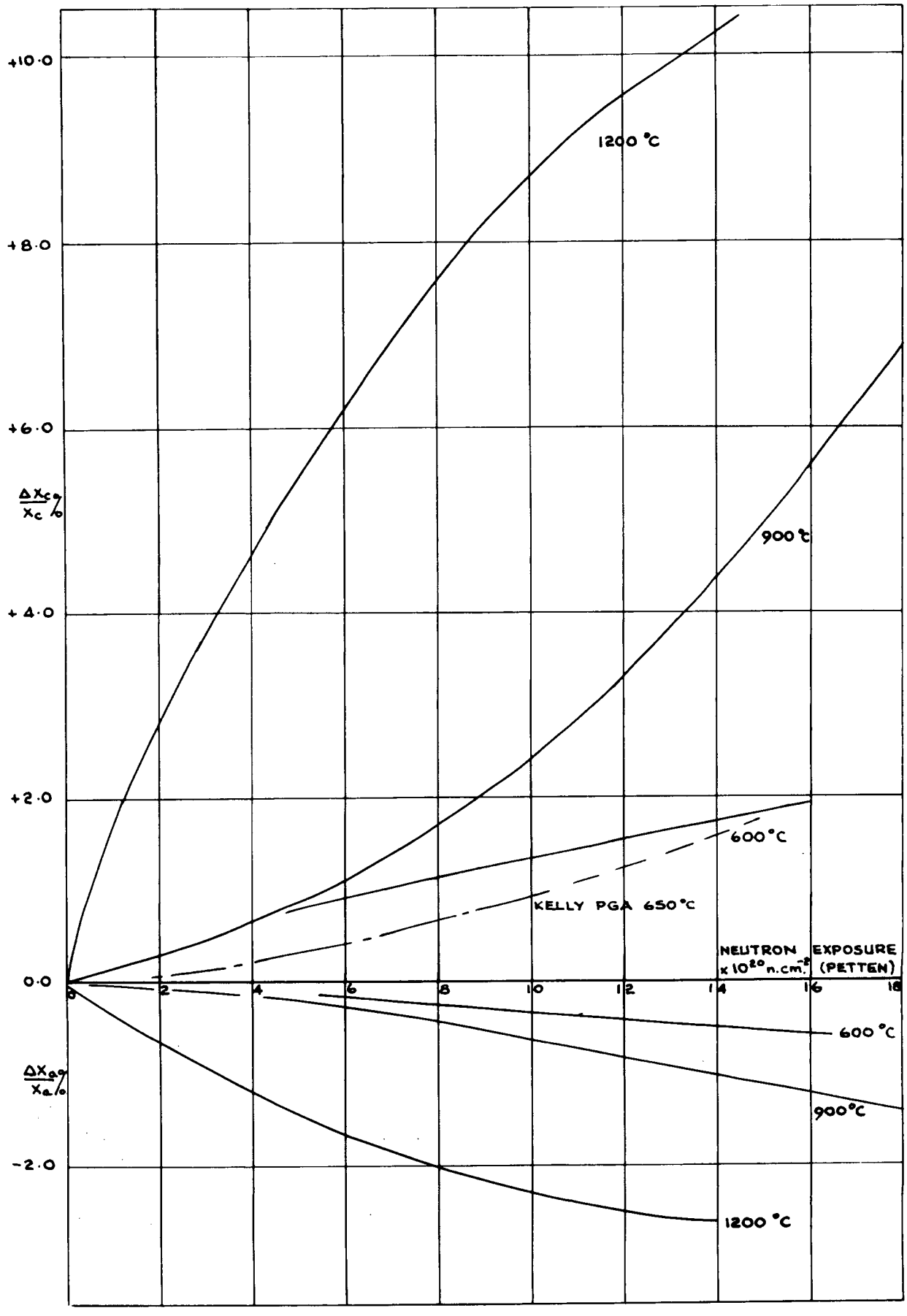

FIG. 21 APPARENT CRYSTALLITE DIMENSIONAL CHANGES CALCULATED FROM GOO BULK DIMENSIONAL CHANGES

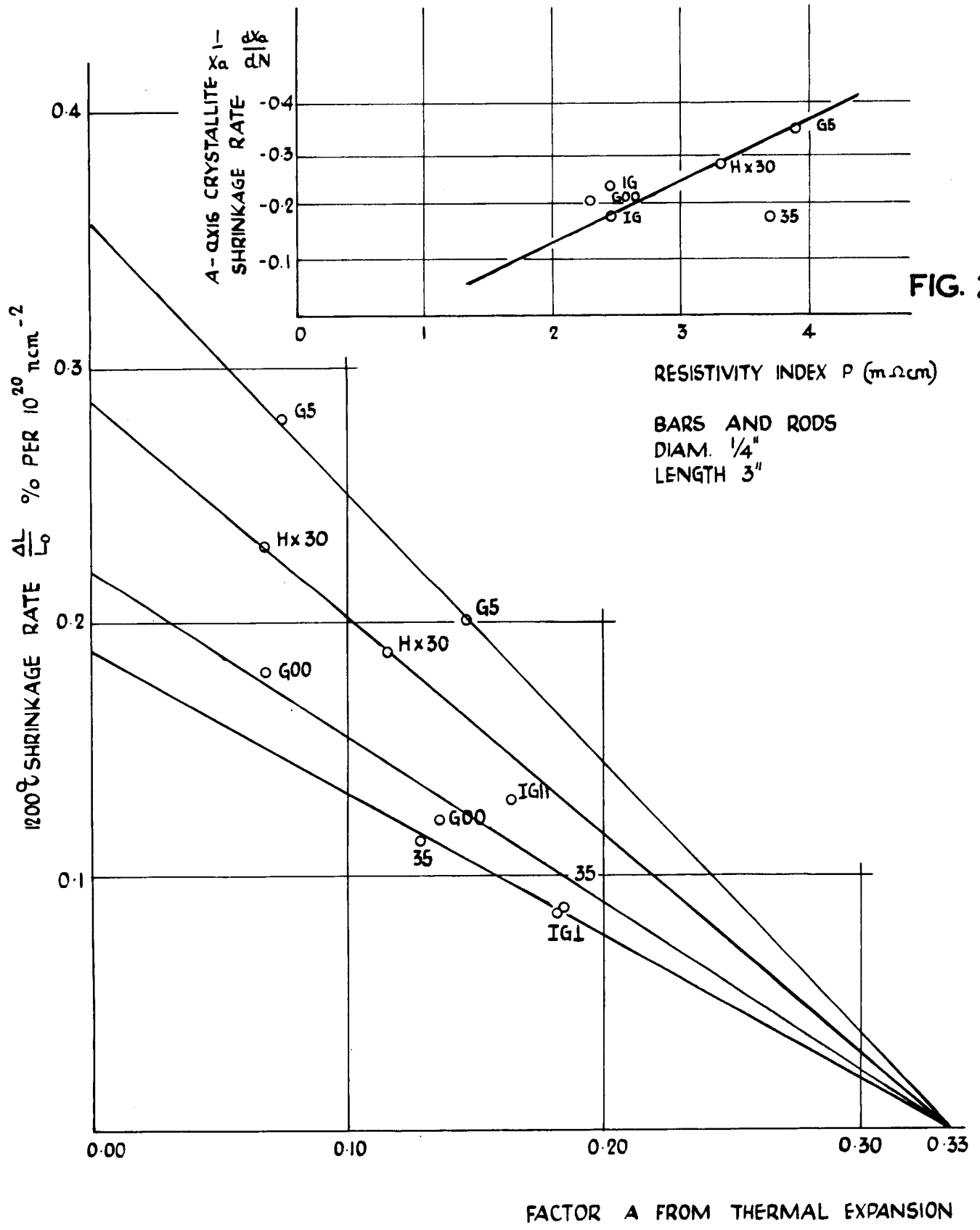

FIG. 22B

FIG. 22A

DERIVATION OF APPARENT BASAL PLANE SHRINKAGE RATE IN CRYSTALLITES OF DIFFERENT GRAPHITES (22A) AND CORRELATION WITH ELECTRICAL RESISTIVITY (22B)

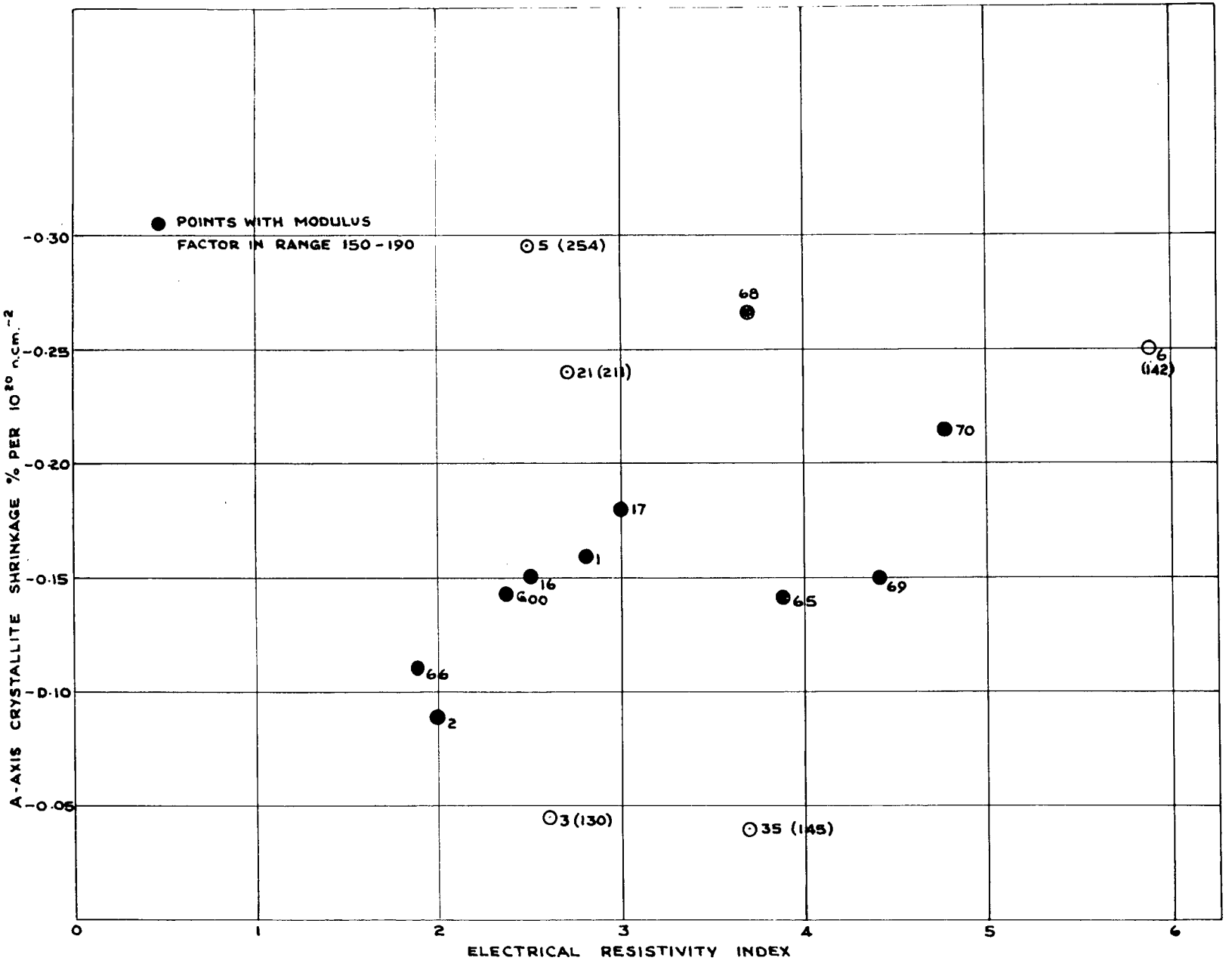

FIG. 23 APPARENT A-DIRECTION CRYSTALLITE SHRINKAGE VERSUS RESISTIVITY INDEX FOR SMALL CUBES AND RODS. (TEMPERATURE 1200 C FIGURES IN BRACKETS ARE RELATED TO YOUNGS MODULUS - SEE TEXT)

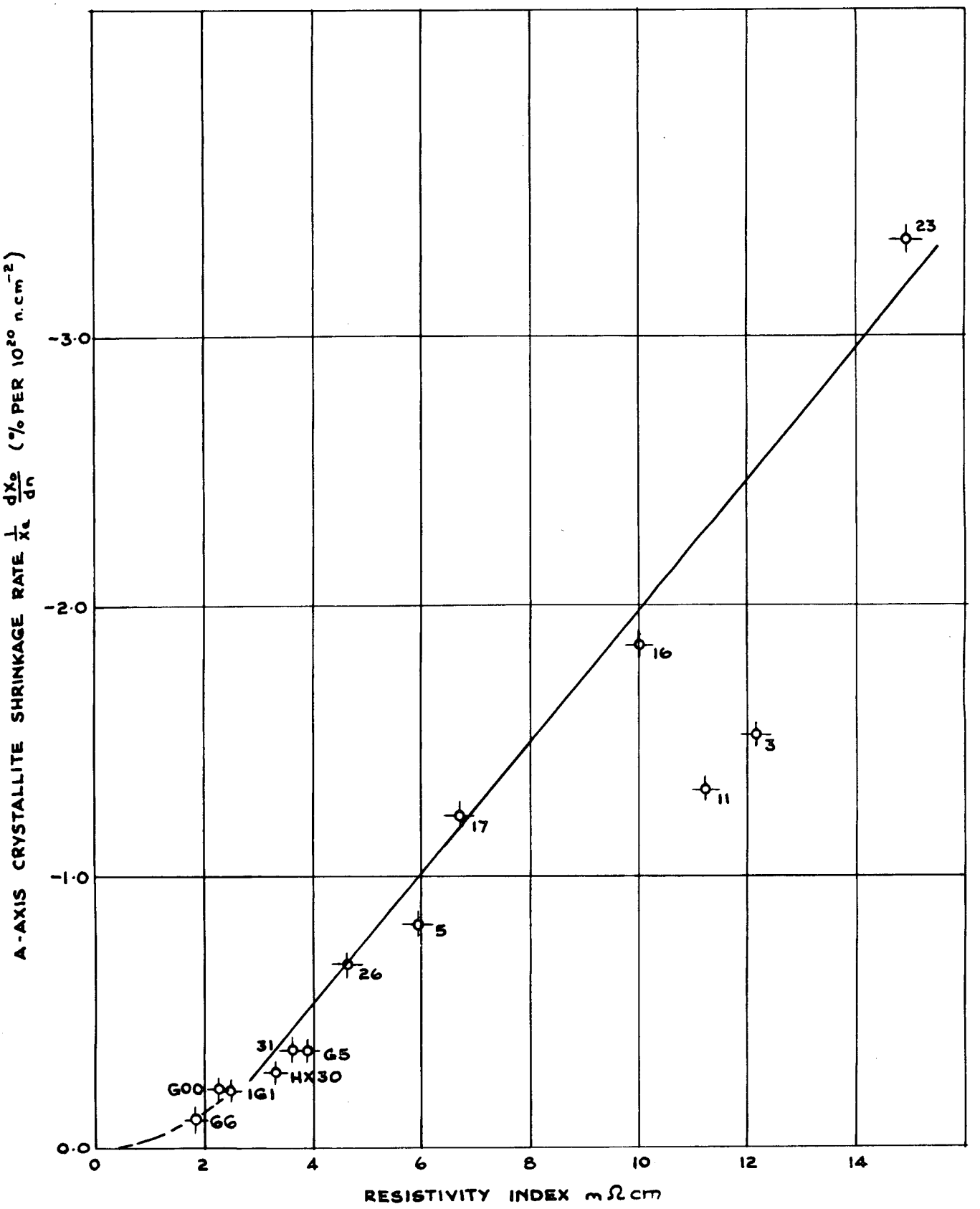

FIG. 24 A-AXIS CRYSTALLITE SHRINKAGE RATE AT 1200 °C VERSUS RESISTIVITY INDEX FOR SOME PYROCARBON DISCS

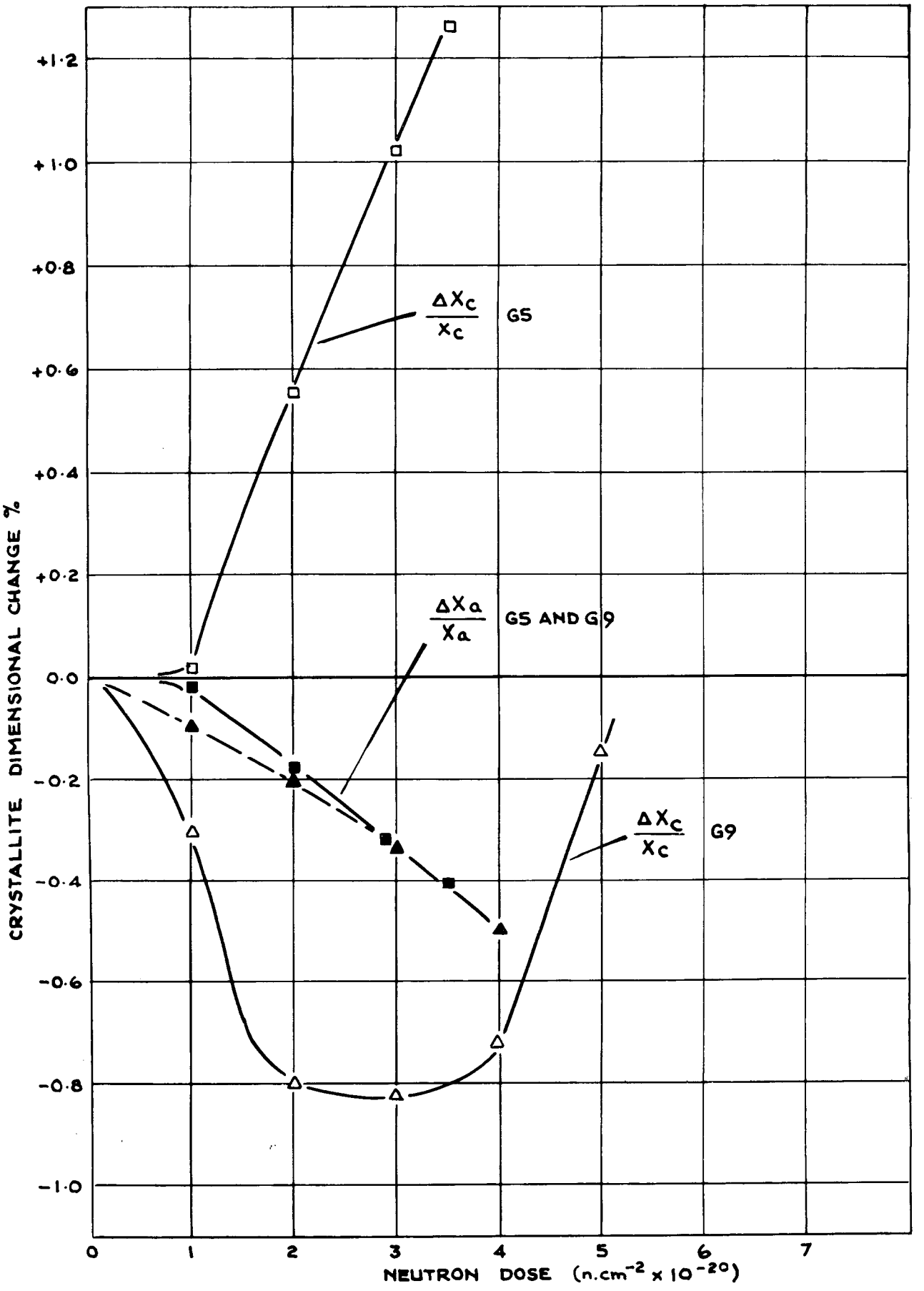

FIG. 25 APPARENT CRYSTALLITE DIMENSIONAL CHANGES AT 900 °C IN G5 AND G9 WITH NEUTRON DOSE

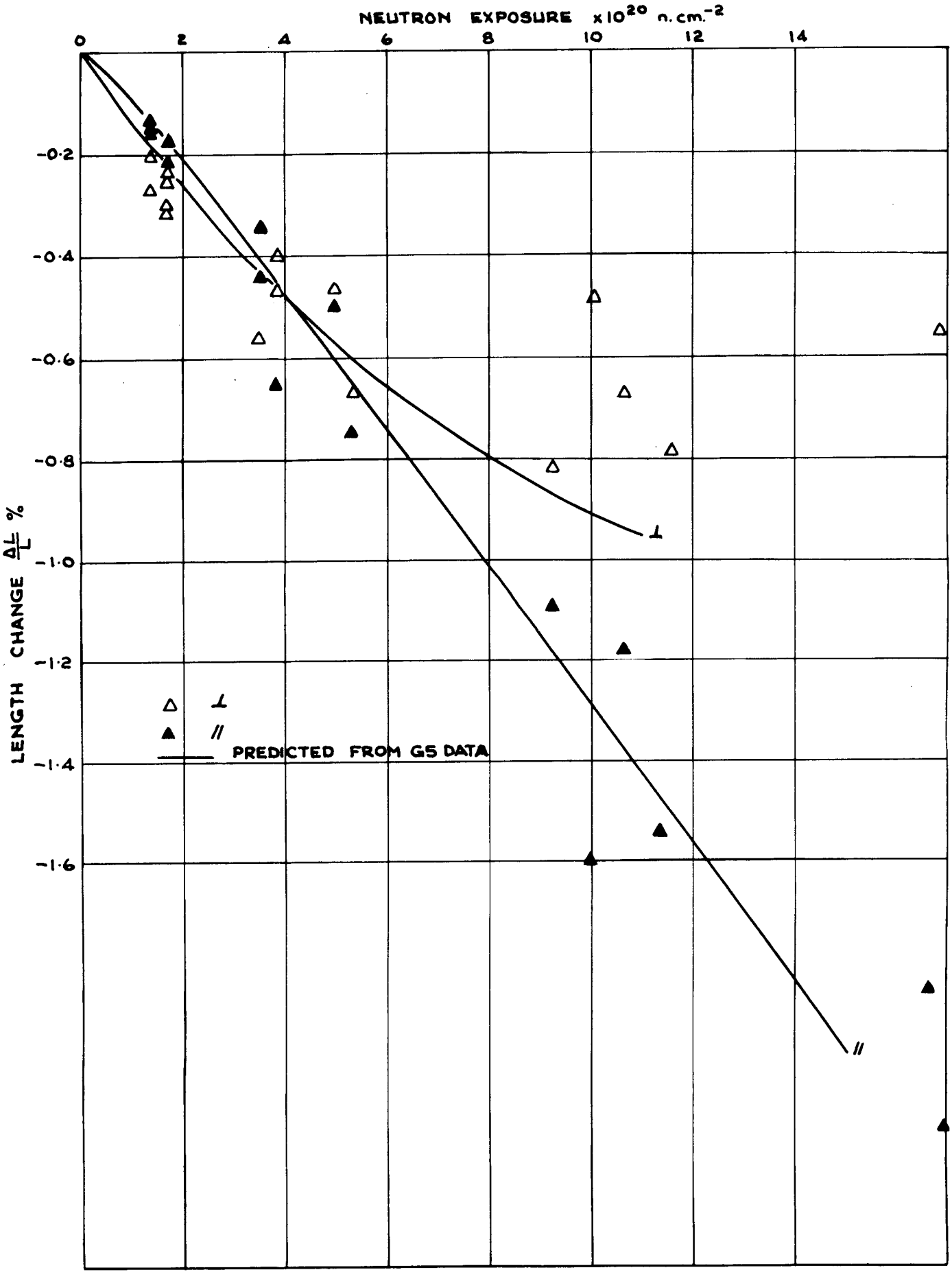

FIG. 26 DIMENSIONAL CHANGES G9 900 °C

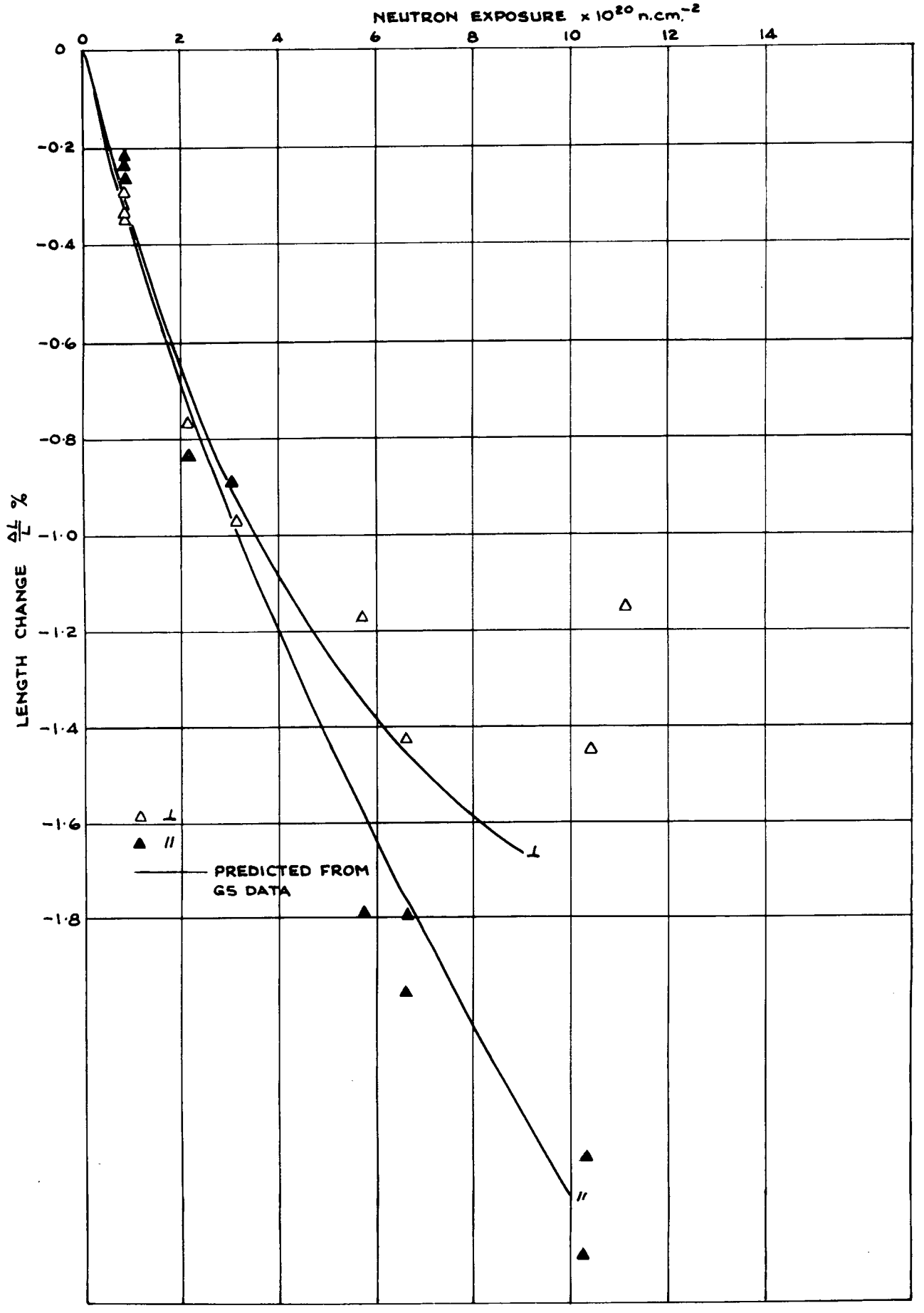

FIG. 27 DIMENSIONAL CHANGES G9 1200 °C

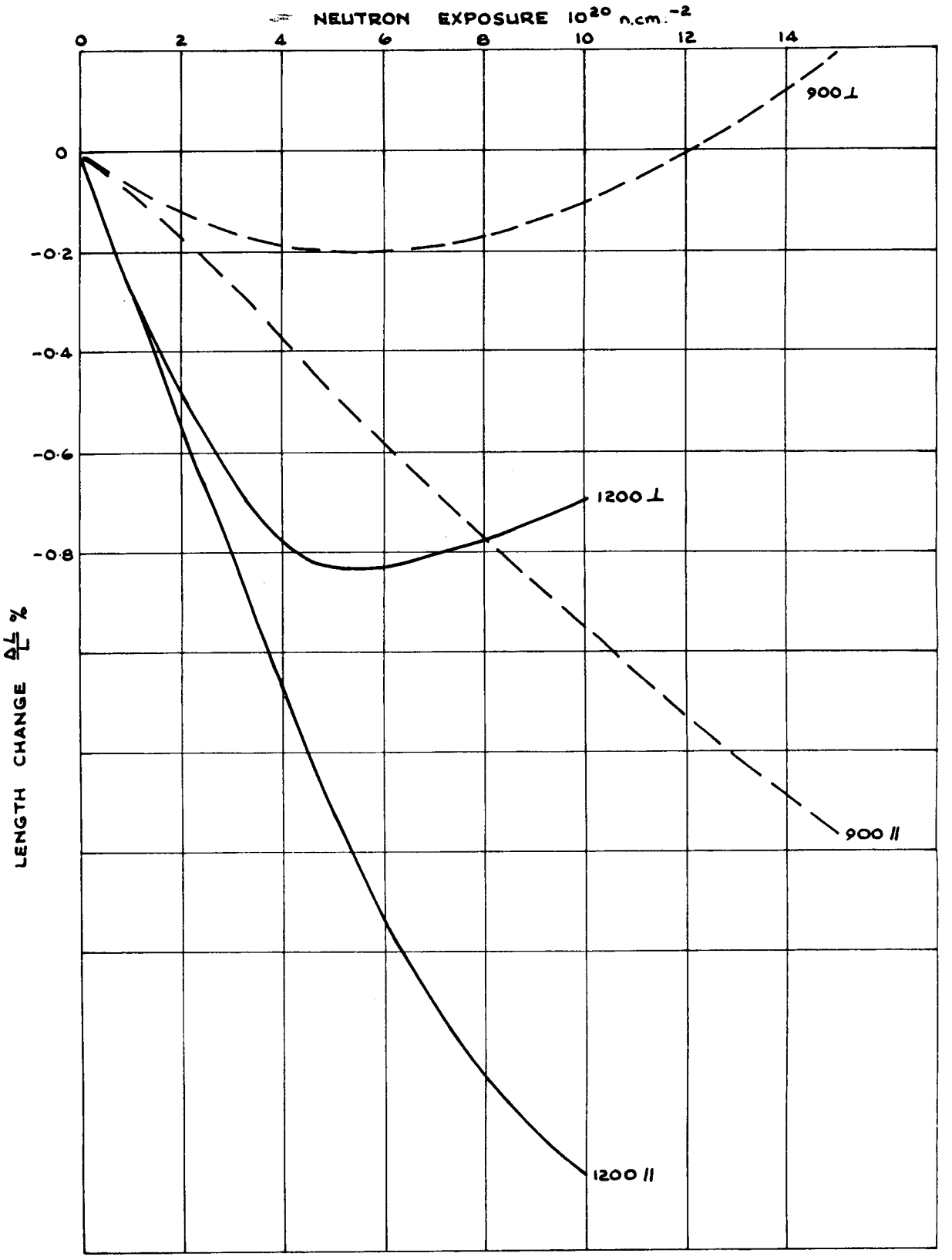

FIG. 28 DIMENSIONAL CHANGES OF STRESS FREE G9